

Submitted to *Astrophys. J.*

A Bayesian Analysis of the Cepheid Distance Scale

Thomas G. Barnes III

McDonald Observatory, University of Texas at Austin, Austin, TX 78712

`tgb@astro.as.utexas.edu`

W. H. Jefferys

Department of Astronomy, University of Texas at Austin, Austin, TX 78712

`bill@astro.as.utexas.edu`

J. O. Berger and Peter J. Mueller¹

Institute for Statistics and Decision Sciences, Duke University, Durham, NC 27708

K. Orr²

Department of Astronomy, University of Texas at Austin, Austin, TX 78712

and

R. Rodriguez³

Department of Astronomy, University of Texas at Austin, Austin, TX 78712

ABSTRACT

We develop and describe a Bayesian statistical analysis to solve the surface brightness equations for Cepheid distances and stellar properties. Our analysis provides a mathematically rigorous and objective solution to the problem, including immunity from Lutz-Kelker bias. We discuss the choice of priors, show the construction of the likelihood distribution, and give sampling algorithms in

¹Now at M. D. Anderson Cancer Center, Houston, TX.

²Now at Baylor University, Waco, TX.

³Now at Northwestern University

a Markov Chain Monte Carlo approach for efficiently and completely sampling the posterior probability distribution. Our analysis averages over the probabilities associated with several models rather than attempting to pick the ‘best model’ from several possible models. Using a sample of thirteen Cepheids we demonstrate the method. We discuss diagnostics of the analysis and the effects of the astrophysical choices going into the model. We show that we can objectively model the order of Fourier polynomial fits to the light and velocity data. By comparison with theoretical models of Bono *et al.* (2001) we find that EU Tau and SZ Tau are overtone pulsators, most likely without convective overshoot. The period-radius and period-luminosity relations we obtain are shown to be compatible with those in the recent literature. Specifically, we find $\log(\langle R \rangle) = 0.693(\pm 0.037)(\log(P) - 1.2) + 2.042(\pm 0.047)$ and $\langle M_v \rangle = -2.690(\pm 0.169)(\log(P) - 1.2) - 4.699(\pm 0.216)$.

Subject headings: cepheid distance scale, bayesian statistics

1. Introduction

Astrophysics is replete with statistical analyses of research problems. Overwhelmingly the approach applied is frequentist. However, in many problems there are advantages to a Bayesian approach. It is coherent and systematic, and in principle it is straightforward to write down all of the elements of even a complex mathematical and statistical model that fairly captures our understanding of the problem. The Bayesian approach is also well-suited to objective selection of an empirical model, such as a Fourier polynomial of unknown order to represent the pulsations of a variable star, from many possible polynomials competing for our attention. It addresses the errors-in-variables problem and the proper handling of errors in the data in a natural way. In this paper we apply Bayesian statistics to a problem of considerable astrophysical interest: the distance scale of Cepheid variables as determined through the surface brightness technique.

The surface brightness technique is widely applied to determination of the Cepheid period-luminosity and period-radius relations. Applications of the method have improved steadily since it was first discussed by Barnes *et al.* (1977) but are still not mathematically rigorous and objective. The essence of the technique is to infer the stellar angular diameter from an appropriate magnitude and color index pair, compare this angular diameter throughout the pulsation cycle with linear displacements of the stellar atmosphere obtained by integrating the radial velocity curve, and extract the mean stellar radius and the stellar distance. To our knowledge none of the published applications objectively selects, as

part of the problem, a model for the radial velocity curve so that it may be integrated. This is straightforward in our Bayesian approach. Secondly, none of the published applications handle propagation of the radial velocity uncertainties through the integration in a mathematically rigorous way. The analysis in our work does so. Finally, both the angular diameters and the linear displacements have error; not all published applications treat this *errors-in-variables* problem correctly. Again, our approach does this naturally.

A second reason to apply rigorous analysis to the surface brightness determination of Cepheid distances is that the Cepheid period-luminosity (PL) relation provides the foundation for the extragalactic distance scale and all conclusions that derive from it. In their final report on the Hubble Space Telescope Key Project on H_0 , Freedman *et al.* (2001) list several difficulties with the Cepheid PL relation, among which is the following “... an accurate geometric calibration of the PL relation, at any given metallicity, has not yet been established.” The surface brightness method has recently been calibrated geometrically through interferometric angular diameters of Cepheids (Nordgren *et al.* 2002). Strong confidence in that calibration arises from its prediction of the same parallax for δ Cep, within $1\% \pm 4\%$, as obtained using the Hubble Space Telescope (Benedict *et al.* 2002). The Nordgren *et al.* (2002) surface brightness calibration permits Cepheid distances to be determined that are very close to, if not fully, geometric and that are fully independent of all other astronomical distance scales. In this work we apply that calibration to a modest selection of Cepheids to gauge its effect upon the Cepheid distance scale.

2. The Surface Brightness Relationship

The visual surface brightness parameter F_v was introduced by Barnes & Evans (1976) as

$$F_v = 4.2207 - 0.1V_0 - 0.5 \log \phi \quad (1)$$

and also,

$$F_v = \log T_e + 0.1BC, \quad (2)$$

where V_0 is the stellar visual magnitude corrected for interstellar extinction, ϕ is the stellar angular diameter expressed in milliarcseconds, T_e is the effective temperature and BC is the bolometric correction. In that paper and in Barnes, Evans, & Parsons (1976) they showed that F_v is tightly correlated with Johnson color index $(V - R)_0$ for a very wide range of stellar types. Specifically for Cepheids, Barnes *et al.* (1977) demonstrated a linear relationship

$$F_v = A + B(V - R)_0 \quad (3)$$

and used this relation to infer a distance scale for Cepheids. The parameters in Eq.(3), called the visual surface brightness relation, and its extension to other photometric bands have been addressed over time by many authors. Discussions of previous work have been given by Fouqué & Gieren (1997) and by Nordgren *et al.* (2002).

Because there had been no high-quality angular diameters of Cepheids until very recently, all attempts to determine the parameters of Eq.(3) have been indirect. One approach has been to assume that the Cepheid surface brightness relation is the same as that for nonvariable giants and supergiants with measured angular diameters, for which Eq.(3) can be calibrated through Eq.(1) (Welch 1994, Fouqué & Gieren 1997). Another method has used the Cepheid temperature and bolometric correction scales to calibrate Eq.(3) through Eq.(2), *e.g.* Gieren, Barnes, & Moffett (1993). Still another approach used model atmosphere calculations for Cepheids to establish the dependence, *e.g.*, Hindsley & Bell (1986) and Gieren, Barnes, & Moffett (1993). Because these approaches established the surface brightness relation indirectly, they are open to criticism that the resultant distance scale may be adversely affected by the assumptions made.

Recently Nordgren *et al.* (2002), used interferometrically determined angular diameters of Cepheid variables to establish the parameters of Eq.(3). Fifty-nine interferometrically measured angular diameters of the Cepheids η Aql, δ Cep and ζ Gem yielded

$$F_v = 3.941(\pm 0.004) - 0.368(\pm 0.007) (V - R)_0 \quad (4)$$

Because Eqs.(4) is based upon measured angular diameters, the surface brightness technique may finally fulfill its original promise: determination of essentially geometric distances to Cepheids. We have adopted Eq.(4) for the analyses in this paper.

3. Cepheid distance determination

As developed by Barnes *et al.* (1977) and extended by Gieren, Barnes, & Moffett (1993), the surface brightness relation permits an independent distance scale to be determined for Cepheids. Those works may be consulted for full discussion; here we give a synopsis of the method to lay the foundation for our Bayesian analysis.

At each time t in the pulsation of the Cepheid, Eqs.(1) and (3) may be combined to obtain the angular diameter variation of the star, $\phi(t)$,

$$4.2207 - 0.1V_0(t) - 0.5 \log \phi(t) = A + B (V - R)_0(t) \quad (5)$$

In addition we infer the Cepheid's linear radius variation $\Delta R(t)$ about the mean radius from

an integration of the radial velocity curve, $V_r(t)$,

$$\Delta R(t) = - \int p(V_r(t) - V_\gamma) dt \quad (6)$$

where the factor $-p$ converts observed radial velocity to the star’s pulsational velocity and V_γ is the center-of-mass radial velocity of the star. Integration of the discrete radial velocity data requires that the velocity variation be appropriately modeled. We follow convention and model the velocity variation as a Fourier series of order M . However, unlike the conventional approach, our Bayesian analysis permits M to be determined as part of the problem, rather than being selected by *ad hoc* means. Indeed, we will go further and average over the best models in an optimal way, thus improving the results over simple selection of the “best model,” when more than one model is in the running. We will similarly model the magnitude variation as a Fourier series of order N in order to obtain mean absolute magnitudes.

The distance s and the mean angular diameter ϕ_0 may be inferred from the solution to

$$4.2207 - 0.1V_0(t) - 0.5 \log(\phi_0 + 2000\Delta R(t)/s) = A + B(V - R)_0(t). \quad (7)$$

where ϕ_0 is in milliarcseconds, s is in parsecs, and $\Delta R(t)$ is in AU. (The factor 2000 converts radius to diameter and arcseconds to milliarcseconds.)

4. Bayesian analysis

We have adopted a Bayesian approach to solve for stellar distance and radius through the surface brightness technique. This has a number of advantages. It is coherent and systematic, and in principle it is straightforward to write down all of the elements of even a complex mathematical and statistical model that fairly captures our understanding of the problem. The Bayesian approach we will use is especially well-suited to the situation at hand, where several empirical models for the pulsations of the star (represented as Fourier polynomials of indeterminate order) are competing for our attention, and we need to choose the best representation in a reasonably objective way. Thus, we are faced with a *model selection* or *model averaging* situation; Bayesian analysis can be used to approach such problems in a systematic way (Hoeting *et al.* 1999). A good introduction to the basic ideas can be found in Loredo (1990).

As usual in Bayesian analysis, we consider the possible *states of nature* x , and encode our uncertainty about the states of nature, before looking at the data, in the form of a prior distribution $p(x)$ on the states of nature. The states of nature include: the different possible models we are considering, the parameters of each model (*e.g.*, Fourier coefficients

and variances peculiar to each model), parameters that are common across models (*e.g.*, the parallax of the star, its linear diameter, and an unknown phase factor representing any systematic difference in phase between the photometry and the velocity data), and perhaps other variables and hyperparameters introduced to complete the model.

This *prior* distribution is multiplied by the *likelihood*, which is the probability $p(d|x)$ of obtaining the particular data d we have observed, conditioning on the data, as a function of the *states of nature* x . This leads to the *Bayesian paradigm*, the posterior probability is proportional to prior times likelihood:

$$p(x|d) \propto p(x) \times p(d|x) \tag{8}$$

As always in Bayesian analysis, the data, once observed, are conditioned upon and *fixed*, and the resulting unnormalized *posterior probability distribution* is a function only of the parameters that represent the states of nature.

It can be argued that (almost) all Bayesian inference amounts to evaluating integrals with respect to the posterior distribution $p(x|d)$. This includes posterior means for point estimates, posterior predictive integrals for prediction, and more. However, in practice it is usually impossible to do the integrals analytically. During the past decade and a half, a different approach has been developed in which the *unnormalized* posterior distribution Eq.(8) can be used directly to generate a large Monte Carlo sample from the posterior distribution. This is implemented by computer simulation. Once we have this sample, we can then derive all our inferences from the sample. Thus, we can derive means, medians and variances of a parameter of interest as sample means, medians, and variances of the parameter in the sample, and can also plot approximations to the posterior distributions of particular parameters as histograms of the sample restricted to the particular parameters in question. In principle, the sample encodes any posterior inference that we might be interested in making.

A number of techniques can be used to generate this sample. The most common are Gibbs sampling and Metropolis-Hastings sampling. These go more generally under the name of Markov Chain Monte Carlo (MCMC), and can be used either separately or in combination to generate the sample as a realization of a Markov chain whose stationary distribution is the target posterior distribution (Smith & Gelfand 1992). Using averages of the Monte Carlo samples we can approximate any desired posterior integral by corresponding ergodic averages. For a practical implementation, an initial burn-in is often discarded to achieve a better approximation. There are infinitely many possible Markov chains that might be cooked up that will generate a sample from the posterior distribution. The art is to devise a Markov chain that samples efficiently and completely, and this is more difficult.

We now describe details of the Gibbs sampling and Metropolis-Hastings algorithm for a generic desired stationary distribution $p(x)$. In the application to posterior integration, this is the posterior $p(x|d)$. To indicate a multivariate state vector we generally write (x, y) , *etc.*

4.1. Gibbs sampling

The idea behind Gibbs sampling (Gelfand & Smith 1990) is that, although we may not be able to draw a sample in all variables simultaneously from a high dimensional distribution, we may nonetheless be able to draw samples from lower-dimensional conditional distributions on groups of variables, conditioned on the current values of all the other variables. (For a tutorial discussion see Casella & George 1992.) For example, we may have a distribution $p(x, y)$ from which we cannot directly draw a random sample, but it may be possible to draw samples from the conditional distributions $p(x|y)$ and $p(y|x)$. In this case, we can construct a Markov chain with the desired joint distribution $p(x, y)$ as its stationary distribution as follows. Start from some arbitrary point (x_0, y_0) in the parameter space. Then draw $(x_1, y_1), (x_2, y_2), \dots$ successively by drawing x_i from $p(x|y_{i-1})$ and then drawing y_i from $p(y|x_i)$. The result is a Markov chain whose stationary distribution is $p(x, y)$. This generalizes to any number of variables, and variables can be sampled in groups as well as singly, *e.g.*, $x|y$ could be multivariate normal and the method would still work.

4.2. Metropolis-Hastings sampling

Sometimes it is not possible to sample from one or more of the conditional distributions, as is done in Gibbs sampling. In such a situation, we can resort to the somewhat more brute-force method of Metropolis-Hastings sampling (Tierney 1994). (Again, for a tutorial, see Chib & Greenberg 1995.) The idea is as follows. Suppose we wish to sample from the probability distribution $p(x)$, where again x may be multivariate. We start at an arbitrary point x_0 , and generate successive samples x_1, x_2, \dots by an appropriate rule. In particular, if the current position is x , we choose a *proposal value* x^* by selecting a random variable from a more-or-less arbitrary *proposal distribution* $q(x^*|x)$. Compute the Metropolis-Hastings ratio

$$\alpha = \min \left[1, \frac{p(x^*)q(x|x^*)}{p(x)q(x^*|x)} \right] \tag{9}$$

Then accept the move to x^* with probability α and remain at x with probability $1 - \alpha$. Thus, we either remain at the current point or move to a new point, with a probability depending on the value of α .

It is possible to mix Gibbs and Metropolis-Hastings steps in the same calculation. Thus, if there is a subset of parameters for which we can effectively sample from the conditional distributions, we may use Gibbs sampling on that subset; the remaining variables may be sampled in Metropolis-Hastings steps, in a so-called *Metropolis-within-Gibbs* scheme.

A good deal of art and experience goes into constructing a good scheme. It is important that the Markov chain mix fast across all regions of the parameter space, that it move easily and freely from one region to another, that it not get “stuck” in one region of the parameter space for long, and so forth. Otherwise, it will take an inordinately long time for the sampling scheme to draw a sample that is useful for making inferences. Devising an effective sampling scheme requires a good understanding of the problem. For example, if the proposal distribution $q(x^*|x)$ is *close* to the actual distribution $p(x^*)$ then the Metropolis-Hastings step will be almost a Gibbs step, since the value of α will be close to 1 and the proposed step will almost always be accepted. Also, it is often more efficient to sample parameters in groups. If, for example, several parameters are highly correlated, then approximate knowledge of the correlation structure can be exploited to sample those parameters efficiently.

4.3. Mathematical model and likelihood function

We have unequally-spaced observations of velocity data $U_i, i = 1, \dots, m$, and photometric data consisting of simultaneously-observed magnitude $V_j, j = 1, \dots, n$ and color index $C_j, j = 1, \dots, n$. We are given standard deviations $\sigma_{U_i}, \sigma_{V_j}, \sigma_{C_j}$. However, we are not very confident of these numbers and take the variances of the data to be given by $\sigma_{U_i}^2/\tau_U, \sigma_{V_j}^2/\tau_V, \sigma_{C_j}^2/\tau_C$, where the *hyperparameters* τ_U, τ_V, τ_C are to be estimated. Let u_i, v_j , and c_j denote the unknown true velocity, magnitude, and color index, respectively. Conditional on u_i, v_j and c_j we assume independent normal distributions

$$\begin{aligned} U_i &\sim N(u_i, \sigma_{U_i}^2/\tau_U) \\ V_j &\sim N(v_j, \sigma_{V_j}^2/\tau_V) \\ C_j &\sim N(c_j, \sigma_{C_j}^2/\tau_C) \end{aligned} \tag{10}$$

The velocity u and photometry (v, c) are periodic functions of the time, and so are functions of the pulsation phase θ where $0 \leq \theta < 1$. An obvious strategy is to represent them as Fourier polynomials of some unknown or selectable order, resulting in a model selection/averaging problem. We need to do this only for u and v , since the colors c are mathematically related to u and v through (Eq. 11) below. M and N are the unknown order of the Fourier polynomials for the \mathbf{U} and \mathbf{V} data, respectively. The polynomials contain $2M + 1$ and $2N + 1$ terms, respectively, including the leading constant terms. Thus

we write

$$\begin{aligned}\mathbf{u} &= u_0 + \mathbf{X}_u \mathbf{a}_u \\ \mathbf{v} &= v_0 + \mathbf{X}_v \mathbf{a}_v\end{aligned}$$

where u_0 and v_0 are the mean velocity and apparent magnitude, \mathbf{X}_u and \mathbf{X}_v are $(m \times 2M)$ and $(n \times 2N)$ design matrices consisting of sines and cosines of multiple angles, evaluated at the phases of the data, and \mathbf{a}_u and \mathbf{a}_v are vectors of Fourier coefficients. Note that the velocity data and photometric data are taken independently, so the phases in general are different. Because the velocity and photometry data are taken at different epochs, there may be an unknown phase error $\Delta\theta$ between the two (due to imperfect knowledge of the period of the star and/or to change in the period between the photometric and velocity epochs).

Expressing Eq.(7) in our statistical nomenclature, we have the nonlinear relationship

$$c_j = \frac{1}{B} (4.2207 - 0.1v_j - A - 0.5 \log(\phi_0 + 2000\Delta R_i/s)) \quad (11)$$

where (A, B) are known constants from Eq. (4), ϕ_0 and s are the mean angular diameter and the distance of the star (both to be estimated), and ΔR_i , the linear radial displacement, is calculated from the \mathbf{a}_u by integrating the velocity term-by-term with respect to the phase. This allows us to write down the likelihood function directly from Eqs. (10):

$$\begin{aligned}p(d|x) &= \prod_{i=1}^m \left[\sqrt{\tau_U} \exp\left(-\frac{1}{2}\tau_U(U_i - u_i)^2\right) \right] \\ &\times \prod_{j=1}^n \left[\sqrt{\tau_V} \exp\left(-\frac{1}{2}\tau_V(V_j - v_j)^2\right) \right] \\ &\times \prod_{j=1}^n \left[\sqrt{\tau_C} \exp\left(-\frac{1}{2}\tau_C(C_j - c_j)^2\right) \right]\end{aligned} \quad (12)$$

Some of the parameters appear in the resulting likelihood function in awkward and nonlinear ways through Eq. (11) that will make straightforward Gibbs sampling impossible. A suitably informed Metropolis-within-Gibbs scheme will be needed.

4.4. Priors

The posterior inference is summarized in the posterior distribution on the following unknown parameters:

- (1) The orders of the Fourier models, M (velocities) and N (V magnitudes).

- (2) The precision hyperparameters τ_U, τ_V, τ_C .
- (3) The mean angular diameter ϕ_0 and the unknown phase error $\Delta\theta$.
- (4) The distance s .
- (5) The intercepts u_0 and v_0 and the Fourier coefficients $\mathbf{a}_u, \mathbf{a}_v$.

The posterior distribution is also indirectly a function of additional hyperparameters introduced below, which define the prior probability model on the Fourier coefficients.

We expect the order of the models to be modest; we choose a uniform prior on the models (M, N) up to some cut-off, and zero beyond.

The precision hyperparameters τ_U, τ_V, τ_C are scale variables. We use standard Jeffreys priors, proportional to the reciprocal of the hyperparameter. Probably we could give them more informative priors but it didn't seem necessary in this case. So

$$p(\tau_U) \propto 1/\tau_U, \quad p(\tau_V) \propto 1/\tau_V, \quad p(\tau_C) \propto 1/\tau_C$$

We take the priors on $\Delta\theta$ and ϕ_0 to be flat (uniform). They are well-determined by the data and we have no real prior information that would override the data.

Failure to take the spatial distribution of the stars into account would result in the distances being affected by the *Lutz-Kelker bias* (Lutz & Kelker 1973). But this can be accounted for automatically by choosing the prior on s based on our knowledge of the spatial distribution of the population of stars (Smith 1999). The spatial distribution of Cepheid variables is known to be flattened with respect to the Galactic plane. There are two recent, observationally-supported, determinations of the exponential scale height z_0 . Luri *et al.* (1999) obtained $z_0 = 97 \pm 7$ parsecs and Groenewegen & Oudmaijer (2000) determined $z_0 = 70 \pm 10$ parsecs. We adopted $z_0 = 70 \pm 10$ parsecs and introduced z_0 as an additional parameter. Our prior on the distance looks like

$$p(s) \propto \rho(s)s^2 ds,$$

where $\rho(s)$ is the spatial density of stars:

$$\rho(s) \propto \exp(-|z|/z_0)$$

with $z = s \sin \beta$, and β is the galactic latitude of the star.

The constant terms u_0 and v_0 get a flat prior. Unlike the terms in sines and cosines, which represent the physics of the pulsations, they are just intercepts reflecting an arbitrary

choice of coordinates. The priors on the periodic Fourier coefficients \mathbf{a}_u and \mathbf{a}_v must be chosen carefully. If our prior is too vague, significant terms may be rejected, but if it is too sharp, overfitting may result. For our models we have used a Zellner G-prior, which is equivalent to a maximum entropy prior (Gull 1988), of the form

$$p(\mathbf{a}|\tau_a) \propto \tau_a^L \exp\left(-\frac{\mathbf{a}'\mathbf{X}'\mathbf{X}\mathbf{a}}{2}\tau_a\right)$$

where \mathbf{a} is the vector of Fourier coefficients, \mathbf{X} is the design matrix of sines and cosines for the problem, $L = M$ or N depending on whether the prior is on the velocity or photometry coefficients, and τ_a is another hyperparameter.

These hyperparameters τ_a (one for velocities, τ_{au} , one for photometry, τ_{av}) also need priors. Since they are scale parameters, one might naively put a $1/\tau_a$ Jeffreys prior on these; however, the resulting posterior distribution would be improper (Gull 1988), so a slight adjustment is required. Thus, we pick a prior on τ_a of the form

$$p(\tau_a) \propto \frac{1}{\tau_a^{3/2}} \tag{13}$$

Strictly speaking there might still be a possibility of obtaining an improper posterior distribution due to the “tail” of this distribution, so some researchers include an exponential damping term; however in our case this is not necessary.

4.5. Sampling strategy

Fortunately, the full conditional distributions for the precision parameters and the hyperparameters are standard χ^2 distributions and so the sampling for these parameters can be accomplished with straightforward Gibbs sampling; that is, these parameters are updated by draws from the respective, complete, conditional posterior distributions.

We use a random-walk Metropolis–Hastings algorithm to sample $\Delta\theta$, ϕ_0 and s simultaneously, using as our proposal distribution a multinormal distribution centered on the currently imputed parameter values, with a variance-covariance matrix that is proportional to the variance-covariance matrix for the linearized least-squares problem for just these three parameters. This means linearizing the logarithm in the expression for c_j (Eq. 11). The idea behind this strategy is that we’ll take longer steps in directions with larger variances and shorter steps in directions with smaller variances, while obtaining good sampling in directions that are not parallel to the axes defined by the parameters, so that if there are significant correlations between these three variables we will still sample them efficiently.

This turns out to have very good acceptance-rejection probabilities and good sampling of the parameter space for these parameters.

The sampling for \mathbf{a}_u and \mathbf{a}_v is more direct. We base our proposal for a Metropolis step on the solution of the linear least squares problems generated by

$$\begin{aligned}\mathbf{U} &\sim \mathbf{N}(u_0 + \mathbf{X}_u \mathbf{a}_u, \sigma_U^2 / \tau_U) \\ \mathbf{V} &\sim \mathbf{N}(v_0 + \mathbf{X}_v \mathbf{a}_v, \sigma_V^2 / \tau_V)\end{aligned}$$

This results in a near-Gibbs sampler for these parameters. It isn't quite Gibbs because of the nonlinear way in which \mathbf{a}_u and \mathbf{a}_v appear in the full likelihood. However, it is very close; the acceptance probabilities for these proposals are over 90%, and the sampling of the Fourier parameter space is very effective. Again, by sampling the parameters simultaneously, we will be able to sample efficiently even if they have significant correlations.

Updating the Fourier coefficients we run into an additional complication. Updating the unknown order of M and N, respectively, of the Fourier approximation requires us to consider MCMC simulation across models of differing dimensional parameter space. For example, if we want to consider incrementing M, we need to add additional coefficients in \mathbf{a}_u . MCMC schemes that allow such moves across different dimension models are known as reversible jump MCMC (Green 1995; Carlin & Chib 1995). See, for example, Dellaportas, Forster, & Ntzoufras (2002) for a tutorial review. We include a reversible jump MCMC move with the steps in \mathbf{a}_u and \mathbf{a}_v . Thus, if the current model has a certain number of parameters, we propose a jump to a model with a (possibly different) number of parameters and simultaneously propose new values for all the Fourier coefficients. To make the sampling efficient, during the burn-in phase we also estimate the posterior probabilities of the individual models. We use this as the basis for the proposal probabilities of new models during the computation phase of the calculation. Thus we will propose models of higher posterior probability with greater frequency.

5. Cepheid data

5.1. Selection of Cepheids

The thirteen Cepheids selected for our analyses were chosen because of their high quality photometry and availability of radial velocities, although one of the velocity curves is of poor quality (RS Pup). The latter permitted testing our analysis with less than ideal data. In addition, we desired a large range in pulsation period, a range in interstellar extinction, and inclusion of possible overtone pulsators (SZ Tau, EU Tau). The Cepheids selected and some

quantities of interest are listed in Table 1. These quantities and the individual stars are discussed in the following subsections.

5.2. Photometry and Radial Velocities

For each Cepheid we require photometric magnitude and color data and radial velocities. These data were collected from the recent literature with much help from the McMaster Cepheid Photometry and Radial Velocity Archive (URL <http://dogwood.physics.mcmaster.ca/Cepheid//HomePage.html>) and from electronic transfers of data by N. Samus and L. Berdnikov.

We chose to use all photometric data for which HJD, V , and $(V - R)$ were available. Photometry acquired in the Cousins $(V - R)_c$ system was converted to the Johnson $(V - R)_j$ system using the precepts of Taylor (1986) as given in his Table 4:

in right ascension zone 01:20–10:00 hours

$$(V - R)_j = ((V - R)_c + 0.035) / 0.714 \quad (14)$$

in right ascension zone 15:30–18:00 hours

$$(V - R)_j = ((V - R)_c + 0.023) / 0.714 \quad (15)$$

for all other right ascension values

$$(V - R)_j = ((V - R)_c + 0.029) / 0.714 \quad (16)$$

These relations shift the zero point of the $(V - R)_j$ scale by ± 0.008 magnitude for Cepheids in the two right ascension zones. This has a negligible effect upon our results. Because all the data in our sample have been transformed, we will hereafter drop the subscript j on the Johnson $(V - R)$.

We used all radial velocity data in the literature published in 1980 and later. The factor, p , that converts radial velocity to pulsational velocity was adopted from Gieren, Barnes, & Moffett (1989a).

$$p = 1.39 - 0.03 \log P \quad (17)$$

where the period P is in days. This relation is an approximation to the theoretical values for Cepheids derived by Hindsley & Bell (1986). The range in p for the Cepheids in this paper is 1.34–1.38, with the lower values of p corresponding to the longer pulsation periods.

We require an uncertainty for each value of V , $(V - R)$ and radial velocity, V_r . The uncertainties in the original sources were adopted when given, estimated when not given, and equated to the previously defined parameters σ_V , σ_C and σ_U , respectively.

In most cases the photometry and velocities were not obtained simultaneously, requiring care in the choice of pulsation period to phase the data properly. The periods listed in Table 1 yielded light, color and velocity curves with no obvious systematic effects between sources, unless otherwise noted.

5.3. Interstellar reddening

$E(B - V)$ values were taken from Fernie *et al.* (1995) as tabulated at URL <http://ddo.astro.utoronto.ca/cepheids.html>. Following the recommendation at that site, we chose the values in column FE1 which are the $E(B - V)^{clus}$ values of Fernie (1990). These reddenings are listed in Table 1.

We took the ratio of total-to-selective absorption, R , from the work of Gieren, Barnes, & Moffett (1993), which was itself adapted from Olson (1975),

$$R = 3.15 + 0.25(< B > - < V >)_0 + 0.05E(B - V) \quad (18)$$

Values of $(< B > - < V >)_0$ were taken from the Fourier fits by Moffett & Barnes (1985). The range of R values for the Cepheids in our sample is 3.28–3.42 with mean 3.35.

With that range of R the Cardelli, Clayton, & Mathis (1989) reddening law gives

$$E(V - R)/E(B - V) = 0.80 \pm 0.02, \quad (19)$$

reasonably close to the ratio 0.84 obtained earlier by Johnson (1968). We have adopted the latter value for consistency with our earlier work.

5.4. Individual Cepheids

In Table 2 we tabulate both the number of observations and the sources of the photometry and radial velocities. In the following we note any peculiarities in the data that required attention.

T Mon — We did not use the photometry of Berdnikov, Ignatova, & Vozyakova (1998) because we could not satisfactorily transform their $(V - R)_c$ to the Johnson system for this star. (In general we were able to transform their photometry successfully; when we were

not, as for T Mon, we note that in the discussion of the individual Cepheids.) We adopted the parameterization of the pulsation period given by Evans *et al.* (1999); *i.e.*, prior to $HJD = 2445700$ the period is 27.019389 days and subsequently, 27.032881 days. In our tables and plots we characterize the period as 27.026 days.

T Mon is the only Cepheid in our sample with a binary orbit. Evans *et al.* (1999) give two acceptable orbits; one with an orbital period of 93987 ± 17972 days and another with 33650 ± 381 days. The orbital contribution to the radial velocity is essentially the same for both orbits over the time span of our analysis. We adopted the longer period orbit and corrected the observed velocities accordingly.

RS Pup — According to Szabados (1999, private communication) the period of RS Pup is highly unstable. We computed a period 41.467 ± 0.002 days from our photometric data set that also fits the relatively poor radial velocity data. This may be compared to the period 41.386 days given by the GCVS1987 and 41.415 days listed by Moffett & Barnes (1985).

U Sgr — U Sgr shows some evidence of binarity in the radial velocities; however, no orbital solution has been found. Using Table 1 of Bersier *et al.* (1994) we attempted a correction for the binary orbit, but this greatly degraded the velocity curve. We chose to ignore the binary correction.

WZ Sgr — The color curve shows some modest systematic differences among the sources, but we did not attempt to address this.

BB Sgr — The shape of the velocity curve differs slightly between Gieren (1981a), on the one hand, and Gorynya *et al.* (1998), Gorynya *et al.* (1996), and Lloyd Evans (1980) on the other. We did not attempt to reconcile the difference.

RY Sco — The $(V - R)_c$ transformation had to be modified to map the Cousins data of Berdnikov & Turner (2000) and Coulson & Caldwell (1985) to the Johnson data of Moffett & Barnes (1984). We changed Eq.(15) to

$$(V - R)_j = ((V - R)_c + 0.043) / 0.714 \quad (20)$$

SZ Tau — The photometric data in Berdnikov, Ignatova, & Vozyakova (1998) and Berdnikov, Ignatova, & Vozyakova (1997) did not satisfactorily transform from $(V - R)_c$ to $(V - R)_j$ and were not used. We computed a new period that fit the photometric data well. Our period of 3.14895 ± 0.00002 days differs by -0.00019 day from that found for earlier epochs by Szabados (1991). Szabados noted that SZ Tau shows erratic period variation larger than the change adopted here. The new photometric period does not fit the full velocity data set, which covers a longer time interval than the photometry. On the other hand, a

best fit period to the velocities does not adequately fit the photometry. To resolve this, we applied our photometrically determined period to both the photometry and the velocities. Then velocities obtained after $HJD = 2447500$ were shifted by $+0.06$ in phase to bring them into phase agreement with earlier velocities.

EU Tau — Photometric data in Berdnikov, Ignatova, & Vozyakova (1998) and Berdnikov, Ignatova, & Vozyakova (1997) did not satisfactorily transform from $(V - R)_c$ to $(V - R)_j$ and were not used. We adjusted the radial velocities of Gieren *et al.* (1989b), as suggested in their paper, by $+3.05$ km/s.

T Vul — We adjusted the radial velocities of Bersier *et al.* (1994) by $+3$ km/s to force agreement with the other velocity data.

SV Vul — The quadratic period given by Szabados (1991) did not fit the current data set. We computed a new ephemeris for the photometric and radial velocity data used here that fits both reasonably. The variation we obtained is

$$HJD_{max} = 2443716.383 + 45.0850E - 0.000600E^2, \quad (21)$$

which may be compared to that of Szabados (1991)

$$HJD_{max} = 2443716.383 + 45.0068E - 0.000364E^2 \quad (22)$$

In our tables and plots we characterize the period as 45.019 days. As Szabados (1991) has noted, the instantaneous period of SV Vul varies about the mean period by several days. This induces a scatter that is readily apparent in our photometric light and color curves.

6. Results

The calculations were run on a Macintosh G4 computer under system MacOS 9.1 using the R-1.4.1 language distributed by the R Development Core Team (See URL <http://www.R-project.org/>). (R-1.4.1 is available for several platforms.) For all stars we adopted a “burn-in” of 1000 samples and a total number of 10,000 samples. Output quantities and their uncertainties are shown in Tables 3, 4 and 7. In this section we discuss these quantities.

6.1. Analysis diagnostics

In Table 3 we list diagnostic parameters, *i.e.* quantities that inform us about the quality of the data and of the analysis. The quantities given are the phase difference between the

photometry and velocities ($\Delta\theta$) and its uncertainty, the most probable number of terms in the V magnitude Fourier model (N), the most probable number of terms in the velocity Fourier model (M), and the square roots of the hyperparameters ($\sqrt{\tau}$) on the photometric and velocity uncertainties. We will discuss these in turn.

6.1.1. Phase shifts

Recall that our model permits a difference in phase ($\Delta\theta$) between the Fourier series model for the photometry and that for the velocity. (The offset $\Delta\theta$ is *added* to the displacement curve phases, thus it is an adjustment to the phases of the velocities relative to the photometry.) $\Delta\theta$ allows for the possibility that we have adopted an incorrect period in phasing the data or that the period has changed between the epoch of the photometry and that of the velocities. It is obvious that an incorrect period, coupled with photometry and velocities acquired at different epochs, would lead to a phase shift between the modeled photometry and the modeled velocities. However, Barnes *et al.* (1977) have shown that an incorrect slope in the surface brightness relation, Eq. 4, can also lead to a non-zero $\Delta\theta$. It is important that we determine whether either of these possibilities is true.

Seven of the thirteen Cepheids show a non-zero $\Delta\theta$, with estimated posterior mean more than two posterior standard deviations away from zero. We will first enquire whether these seven may be the result of period errors. If the adopted period is incorrect or has changed, we expect a significant $\Delta\theta$ value to arise when the photometry and the velocities are not coeval. To test this we computed for each of the seven Cepheids the mean date of the photometric observations, the mean date of the velocity observations, and the change in period required to account for the $\Delta\theta$ listed in Table 3 over that interval. For five of the stars (excluding X Cyg and BF Oph) the change in period required to account for $\Delta\theta$ is comparable to the uncertainty in the period. In most of these cases the fault is not so much a poor period, as a large interval between the photometry and the velocities given the period uncertainty. For these five we attribute the apparently significant $\Delta\theta$ to uncertainty in the period coupled with a large interval between the photometric observations and the velocity observations.

For X Cyg and BF Oph, the required change in period is seemingly much larger than the uncertainty in the period will support. In the case of X Cyg, Evans (1984) has shown that systematic phase shifts as large as 0.02 period occur. While the origin of these phase shifts is unknown, they may account for the -0.021 phase shift we find over the 85 cycles (nearly 4 years) that separate the photometry and the velocities. For BF Oph the period analysis by Szabados (1989) showed some systematic effects in the residuals, but they are much smaller than the $\Delta\theta$ found in our analysis. An explanation for the large $\Delta\theta$ for BF

Oph that is based on an incorrect period is not supported by Szabados’ analysis.

Thus we find for twelve of the thirteen Cepheids $\Delta\theta$ values that are zero within their uncertainties or have significantly non-zero values that may be attributed to a large gap between the photometric observations and the velocity observations. The phase shift for BF Oph is unexplained. We conclude that the $\Delta\theta$ values found here give us no reason to believe that the adopted slope in the surface brightness relation, Eq. 4, is incorrect.

Nonetheless, this is such an important issue that we will enquire whether the mean $\Delta\theta$ is consistent with the published uncertainty in the slope of the surface brightness relation. The variance weighted mean $\Delta\theta$ for all thirteen stars is -0.0115 ± 0.0065 (s.e.m). Were we to discard the six stars with $\Delta\theta$ values likely affected by non-coeval photometry and velocities, the mean would be -0.0034 ± 0.0099 . A simulation published by Barnes *et al.* (1977) suggests that $\Delta\theta$ of order -0.01 would be caused by a change in the slope of the surface brightness relation of order 0.006 – 0.010 . We ran simulations on all our stars and found that a phase difference of -0.011 results from a change in the slope of -0.012 . With a mean phase shift in the range -0.0034 to -0.0115 , the implied error in the slope in Eq. 4 is -0.004 to -0.013 with the former value being more likely because of changing or erroneous periods. Recall that the uncertainty in the slope of the surface brightness relation, Eq.4, is ± 0.007 , as given by Nordgren *et al.* (2002). We conclude that the phase shifts found here are consistent, within the error, with the adopted slope in Eq.4.

6.1.2. Fourier Polynomial Orders

As discussed in Section 4.3 we modeled the V light curve and the radial velocity curve of each Cepheid as Fourier polynomials of order N and M , respectively. In about half the cases only one polynomial order had a significant posterior probability and that order is listed in Table 3. When multiple orders are listed, the posterior probability is above 5% for all those orders, and they are listed in descending order of the posterior probability. In this section we demonstrate that our analysis reasonably models these curves.

We first demonstrate that our Bayesian analysis chooses a model-based Fourier order that agrees with the order that a researcher would have chosen from exploratory data analysis of the Fourier polynomial against the data. One way to demonstrate this is to compare the orders selected in our analysis with the orders chosen by the traditional method. In the traditional analysis the order is selected based on a visual impression of the fit to the data, usually with the criterion that the polynomial be terminated when the scatter about the polynomial approaches the uncertainty in the data. Note that, because the light and

velocity curves are in reality not finite Fourier series, fitting until the noise level is reached may overfit the curves and lead to excessively large values of N and M .

Moffett & Barnes (1985) have published Fourier series coefficients for the light curves for twelve of our thirteen stars. A Fourier fit for the light curve of the thirteenth star, EU Tau, has been published by Gieren *et al.* (1990). In Figure 1 we plot the order of the V magnitude Fourier polynomial determined here against the order determined in the works just cited. In some cases our results give a significant posterior probability for two values of N ; in those case we have plotted a fractional N determined by weighting by the posterior probabilities. The agreement is excellent, especially when one considers the additional photometry included in our analyses that was not available to the earlier researchers and the possibility of overfitting in previous work. We conclude that the Bayesian analysis successfully and objectively choses the order of the Fourier polynomial for the V magnitude data and therefore for the velocity data also.

Another way to demonstrate the success of our objective order selection is to plot the Fourier polynomial for that order with maximum posterior probability against the data and perform the customary ‘eye ball’ test. The posterior probabilities for the photometry and velocity models for X Cyg are shown in Figures 2 and 3. For the photometry both the ninth and tenth order models are supported by the data. For the velocities, eighth, ninth and tenth order models are supported. In Figures 4 and 5 we show comparisons of the data with Fourier polynomials of order nine. The comparisons are quite reasonable, given that there is significant posterior probability for models with order ten (photometry) and orders eight and ten (velocities).

6.1.3. Hyperparameters τ

Earlier we introduced hyperparameters on the photometric and velocity uncertainties, *i.e.*, we chose not to trust the uncertainties published or adopted for the individual data, and we modeled the extent to which the uncertainties describe the actual scatter in the observations. The hyperparameters τ are defined such that the posterior variances in velocity, in V magnitude, and in $(V - R)$ color data are given respectively by $\sigma_{U_i}^2/\tau_U$, $\sigma_{V_j}^2/\tau_V$, $\sigma_{C_j}^2/\tau_C$ where the σ values are the published or adopted uncertainties. Therefore $\tau \leq 1$ implies that the actual variance of the data about the Fourier polynomial fit is greater than the variance given by the adopted uncertainties.

As shown in Table 3, this is overwhelmingly the case. There we show the mode of each posterior probability distribution for the hyperparameters. (In Table 3 we actually

quote $\sqrt{\tau}$ as it is more closely related to the published standard errors.) Either the adopted uncertainties underestimate the actual scatter in the data, or there is additional scatter in our photometric and velocity curves not represented by the observational errors. (To some extent this may be caused by model misspecification, *i.e.*, we know that these pulsation curves are not finite Fourier series.) Additional scatter could be induced by period jitter affecting the pulsation phases, by errors in the transformation from Cousins-to-Johnson photometry, by mis-matches between the photometric and velocity systems of the original sources, *etc.*

Period jitter is clearly seen in our magnitude and velocity curves for SV Vul. This is a result of unexplained, short time scale variation in the pulsation period, as noted in Section 5.4. It is the likely cause of SV Vul having the smallest τ_U and the next to smallest τ_V . No other star shows evidence of period jitter in examination of the photometry and velocities.

Were the dominant contributor to the excess scatter the Cousins-to-Johnson transformation, the largest effect would be seen in $(V - R)$, as only the color data are affected by the transformation. Just the opposite is seen; $\sqrt{\tau_C}$ is generally larger than the other two. We conclude that our color transformation is not a significant source of additional scatter.

Examination of the individual stellar values of σ_V and σ_C reveals that the claimed observational uncertainties are quite small. For example, the mean values for 330 magnitude and color observations of U Sgr are ± 0.016 mag. and ± 0.018 mag., respectively. In our experience it is quite difficult to achieve such precision in the Johnson magnitudes, especially for large-scale observational programs such as those from which we drew the data for this paper. Furthermore, it is well known that photometric magnitudes are less precise than photometric colors, when obtained with photoelectric photometers, due to cancellation of some error sources in determining the color. That is not borne out in most of these data. Examination of the values of $\sqrt{\tau_C}$ and $\sqrt{\tau_V}$ shows that the color hyperparameter is closer to unity than the magnitude hyperparameter in twelve of thirteen cases. These facts suggest that a reasonable interpretation of the τ values is that the published or adopted uncertainties in the photometry are underestimated. Adopting this interpretation and the values in Table 3, we estimate that the true observational scatter for U Sgr is typically $\sigma_V/\sqrt{\tau_V} = \pm 0.030$ mag. and $\sigma_C/\sqrt{\tau_C} = \pm 0.024$ mag. These are reasonable values for observational programs of the type listed in Table 2. While we cannot rule out all possible sources of excess scatter in the photometric and velocity curves, we believe that underestimated observational uncertainties are the most likely explanation for $\sqrt{\tau} \leq 1$.

6.2. Radius results

In this section we present our results on the radii and angular diameters. Table 4 lists the mean stellar radius ($\langle R \rangle$) in solar radii and the mean stellar angular diameter ($\langle \phi \rangle$) in milliarcseconds, and their uncertainties. Angular diameters are included here for the benefit of researchers making direct measurement of Cepheid angular diameters. The mean uncertainty in a radius is $\pm 7.7\%$, and without the two outliers RS Pup and SZ Tau, it reduces to $\pm 6.5\%$.

A least-squares fit to our results, weighted by the variance in $\log(\langle R \rangle)$ and excluding SZ Tau and EU Tau as possible overtone pulsators, gives the fundamental-mode period-radius (PR) relation from 11 Cepheids

$$\log(\langle R \rangle) = 0.679(\pm 0.050)(\log(P) - 1.2) + 2.044(\pm 0.065), \quad (23)$$

We have placed the zero point of the PR relation at $\log P = 1.2$, at the mid-point of our distribution of periods. Alcock *et al.* (1995) have determined the ratio between first overtone and fundamental period for Galactic Cepheids, which is 0.702 and 0.707 for SZ Tau and EU Tau, respectively. If we include SZ Tau and EU Tau in the PR relation with their equivalent fundamental-mode periods, we obtain for 13 Cepheids

$$\log(\langle R \rangle) = 0.693(\pm 0.037)(\log(P) - 1.2) + 2.042(\pm 0.047), \quad (24)$$

In anticipation of the discussion below of the pulsation status of SZ Tau and EU Tau, we will adopt this as our best estimate for the PR relation and show it in Figure 6.

The weighted rms scatter in Figure 6 is $\sigma = 0.040$, compared to the typical scatter in the $\log \langle R \rangle$ values of $\sigma = 0.033$. This implies an additional scatter in the PR relation of about ± 0.02 . Excess scatter of this order or more is typically found in Cepheid PR relations (see citations in Table 5).

In Table 5 we collect recent determinations of the Cepheid PR relation. We have adjusted these relations to our definition of the factor p given in Eq. 17. We have also recomputed the uncertainties in some cases. The weighted mean PR relation from Table 5 is

$$\log(\langle R \rangle) = 0.690(\pm 0.018)(\log(P) - 1.2) + 1.979(\pm 0.006), \quad (25)$$

(In assigning a weight to the result from theoretical models, we set the uncertainty to a median value so that solution would not dominate the mean.)

It is apparent from the consistent values of the zero point in Table 5 that all methods yield the same radius for a Cepheid of period near 16 days ($\log P = 1.2$). With regard to the

slopes, however, there is much variation in the results. It is beyond the scope of this paper to resolve that question, but it warrants further investigation.

Bono *et al.* (2001) have computed theoretical PR relations for first overtone pulsators; with, and without, convective overshoot. Table 6 compares our observed radii (Table 4) for EU Tau and SZ Tau with those predictions and with the fundamental-mode PR relation (Eq. 25). Our radii are more consistent with overtone pulsation than with fundamental-mode pulsation for both stars. For EU Tau our observed radius supports first overtone pulsation without convective overshoot. While our radius for SZ Tau agrees with that predicted for overtone pulsation without convective overshoot, the larger uncertainty on its radius precludes exclusion of the convective overshoot radius.

6.3. Distance results

In this section we present our results on distance and parallax. Table 7 lists the stellar distance (s) in parsecs, the stellar parallax (π) in milliarcseconds, the magnitude-mean absolute magnitude ($\langle M_V(mag) \rangle$), and the intensity-mean absolute magnitude ($\langle M_V(int) \rangle$), and their uncertainties. The mean uncertainty in distance is $\pm 7.7\%$, and without the two outliers RS Pup and SZ Tau, it reduces to $\pm 6.3\%$. These percentage uncertainties are essentially the same as those in the radii, as expected. The mean uncertainty in absolute magnitude is ± 0.165 mag. in accord with the mean distance uncertainty.

We illustrate the posterior probability distributions for the parallax and distance of T Mon in Figures 7 and 8. It is apparent that the parallax probability distribution is symmetric and that the distance probability distribution is skew. This is to be expected as the two quantities are related through the reciprocal. This means that our results in Table 7 for distance and parallax cannot be related exactly through the reciprocal as each is drawn from its own posterior probability distribution. Our quoted values are the expectation values from those distributions. The skewed nature of the posterior probability distribution in distance will not be found in analyses based on standard maximum-likelihood techniques and shows an advantage of our Bayesian approach.

Figure 9 shows the simulation history of the parallax, demonstrating good acceptance rates for the proposals. There is no evidence of ‘sticking’ or of systematics in the sampling. Figure 9 demonstrates that our proposals have been sampled efficiently and completely. Simulation histories on the other parameters are quite similar.

Figure 10 shows the period-luminosity (PL) relation for our $\langle M_v(int) \rangle$ results. A solution weighted by the variance in $\langle M_v(int) \rangle$ yields, for the eleven fundamental-mode

Cepheids,

$$\langle M_v(int) \rangle = -2.682(\pm 0.215)(\log(P) - 1.2) - 4.699(\pm 0.280) \quad (26)$$

If we include EU Tau and SZ Tau in the calculation with their equivalent fundamental-mode periods, we obtain for 13 Cepheids

$$\langle M_v(int) \rangle = -2.690(\pm 0.169)(\log(P) - 1.2) - 4.699(\pm 0.216) \quad (27)$$

We adopt this as our best estimate for the PL relation and show it in Figure 10.

The weighted rms scatter in Figure 10 is $\sigma = 0.186$ mag. which may be compared to typical uncertainty in Table 7, $\sigma = 0.165$ mag. This indicates an additional scatter in the PL relation of order ± 0.09 mag. beyond that present in our distance determinations. We attribute the additional scatter to the presence of errors in the adopted interstellar extinction corrections and to the fact that the PL relation is an approximation to a period-luminosity-color relation and thus has a cosmic width.

In Table 8 we collect recent determinations of the Cepheid PL relation. Where appropriate we have adjusted these relations to our definition of the factor p given in Eq. 19. (The relation attributed to Turner & Burke (2002) has been computed by us from the 23 $(M_v)_{BW}$ values in their Table 3.) The weighted mean PL relation from Table 8 is

$$\langle M_v(int) \rangle = -2.851(\pm 0.056)(\log(P) - 1.2) - 4.812(\pm 0.058) \quad (28)$$

Eqs. 27 and 28 may be compared to the PL relation adopted by Freedman *et al.* (2001) for the final results of the HST key project on the extragalactic distance scale:

$$\langle M_v \rangle = -2.760(\pm 0.030)(\log(P) - 1.2) - 4.770(\pm 0.030) \quad (29)$$

It is important to compare the predictions of these relations with the absolute magnitude inferred from the Hubble Space Telescope parallax of δ Cep (Benedict *et al.* 2002) and with the absolute magnitude computed from the distance to δ Cep determined by Nordgren *et al.* (2002). (We have adjusted the Nordgren *et al.* distance to our adopted value of p .) The comparisons are listed in Table 9. Given that these values are based on different techniques with different interstellar extinction assumptions, it is remarkable how well they agree with the HST parallax. In particular, our value agrees nicely with the HST value.

6.4. Astrophysical diagnostics

In this section we examine the effects of several astrophysical choices on our results. We test the choice of Galactic scale height for the Cepheid distribution in our prior on distance,

the effect of interstellar reddening errors on the results, and the effect of permitting a phase shift between the velocities and photometry.

As discussed in Section 4.4 we chose a prior on the distance that depends on the scale height of the Cepheid distribution. The two observationally supported choices were $z_0 = 97 \pm 7$ parsecs obtained by Luri *et al.* (1999) and $z_0 = 70 \pm 10$ parsecs from Groenewegen & Oudmaijer (2000). We selected the latter value. We tested this choice by running the analysis on SZ Tau with the alternate value of z_0 . SZ Tau has $distance * \sin(\beta) = -180$ parsecs, the largest $|z|$ in our sample. The result is that distance, radius, and $\Delta\theta$ change by -3 parsecs ($.03\sigma$), -0.2 solar radii ($.03\sigma$), and -0.0027 ($.12\sigma$) pulsational period, respectively, which are entirely negligible compared to the uncertainties. The specific choice of Galactic scale height, within reasonable bounds, does not affect our results. However, including it is crucially important as discussed in section 4.4.

One of the advantages of the visual surface brightness method is its insensitivity to errors in the adopted interstellar reddening. This is easily demonstrated through Eq. 5 with A, B set to their values in Eq. 4 and with the reddening explicitly included in the V_0 and $(V - R)_0$ terms. The prediction is that an error of $+0.10$ mag. in the value of $E(B - V)$ leads to an error of $+1.1\%$ in the angular diameter. The errors in mean radius and distance are related to the error in angular diameter by

$$\delta\phi/\phi = \delta \langle R \rangle / \langle R \rangle - \delta s/s \quad (30)$$

We tested the prediction by running our analysis on RY Sco with an assumed $E(B - V) = 0.877$ rather than the actual value of $E(B - V) = 0.777$. The resulting angular diameter, radius, and distance change by 0.4% , 0.6% , and 0.2% , respectively. While the angular diameter change is somewhat smaller than the prediction, all three are satisfactorily small and are related in accord with Eq. 30. For comparison, note that an error in $E(B - V)$ of $+0.10$ mag. leads to an error in the distance determined through the Cepheid PL relation of -17% . Of course absolute magnitudes determined from visual surface brightness distances contain the full effect of any errors in the reddening.

Finally, we examine the effect of $\Delta\theta$ on our results. Use of such a phase shift permits correction for erroneous or changing periods as we discussed earlier. It has been suggested that a non-zero $\Delta\theta$ may bias the distance results (Laney 1999, private communication). It is important to ascertain whether this occurs. To determine the extent to which our results depend on use of a variable $\Delta\theta$, we modified the analysis to adopt phase agreement between the photometric and velocity data and performed the analysis again on our sample of Cepheids. In Figure 11 we plot the new distances against the distances with $\Delta\theta$ allowed to vary (from Table 7). The distances with $\Delta\theta = 0$ are found to be $0.4\% \pm 0.6\%$ larger in the mean than those with $\Delta\theta = \text{variable}$. It is clear that the use of variable $\Delta\theta$ has not

materially affected the distance results. The test had a similar result for effects upon the mean radius.

6.5. Discussion and Conclusions

We have constructed a fully Bayesian statistical approach to the determination of Cepheid variable star properties through the surface brightness method. This approach obtains a mathematically rigorous solution to the problem, a significant improvement on previous attempts. We have shown how priors that represent our knowledge before looking at the data may be chosen and how the likelihood for the available data may be constructed. The posterior is then the product of the prior distribution and the likelihood. Our analysis makes use of Markov Chain Monte Carlo simulation to generate posterior Monte Carlo samples that can be used to evaluate any desired posterior integral. We have presented an implementation of Gibbs sampling and of Metropolis-Hastings sampling of the posterior distribution so that the distribution may be sampled efficiently (shorter computing times) and completely (reliable inferences).

To demonstrate the Bayesian approach, we applied it to thirteen Cepheids for which appropriate data exist in the literature. The data required for our calculations are Johnson VR photometry, radial velocities, interstellar extinction estimates, and stellar pulsation periods. These were drawn from the literature, although we adjusted the pulsation periods for several stars.

We chose to use the visual surface brightness relation in this test, although our analytic approach may be used on other surface brightness relations, *e.g.* the infrared relation. The relation adopted is one recently calibrated by Nordgren *et al.* (2002) through interferometrically determined angular diameters of several Cepheids. They applied this calibration to the determination of the distance to δ Cep, 272 ± 6 pc. The accuracy of their distance scale has been tested by Benedict *et al.* (2002), who determined the distance to δ Cep 273 ± 9 pc through a Hubble Space Telescope parallax. The $1\% \pm 4\%$ agreement between these distance scales gives us considerable confidence in the Nordgren *et al.* surface brightness relation. (When Nordgren *et al.*'s distance is adjusted to our adopted value of p , the agreement is $4\% \pm 4\%$.) Distances determined in our work with this visual surface brightness relation are therefore very close to, in not on, a geometric distance scale.

Built into our Bayesian approach are numerous opportunities to check the analysis, both analytical and astrophysical checks. We discussed several of these: the phase difference between the photometry and the velocities, the orders of the Fourier series used to model

the photometry and the velocities, hyperparameters on the observational uncertainties, the choice of scale height for the Cepheid distance distribution, the effect of interstellar reddening on our results, and the effect of permitting a phase shift on the distances and radii obtained. In the next few paragraphs we describe these checks on our results.

As part of our analysis, we determined phase shifts that optimally match the photometric and the radial velocities curves. All of these were found to be small, but about half were significant compared to their uncertainties. In six of the seven significant cases we show the $\Delta\theta$ value to be a result of period uncertainty coupled with a significant interval between acquisition of the photometry and the velocities. Because an erroneous slope in the surface brightness relation can create phase shifts similar to those we found, we examined that issue as well. We showed that our phase shifts, if interpreted this way, imply a change in the slope of the surface brightness relation less than its uncertainty.

We also showed that our model-based orders of the Fourier polynomial fits to the light curve (N) and the radial velocity curve (M) agree with previously determined (subjectively chosen) values and that they produce fits to the curves that agree with our (subjective) judgement. The ability to determine N , M objectively is an important feature of our Bayesian approach, as is the ability to average over models with different N or M , each with significant posterior probability.

Because we were unsure that the published observational uncertainties are correct, we introduced hyperparameters into our model to check them. The hyperparameters show clearly that there is more scatter in the light, color, and velocity curves than can be explained by the published observational uncertainties. We examined several possibilities and concluded that the observational uncertainties are likely to be underestimated.

Our analysis takes into account the spatial distribution of Cepheids in a natural way through the choice of distance prior. This means that our distances and absolute magnitudes are not subject to Lutz-Kelker bias. We modified our choice for the scale height of the Cepheid Galactic distribution to enquire whether the specific choice affects our results. We found that a change from 70 ± 10 pc to 97 ± 7 pc, two recent determinations, has a negligible affect upon our distances and radii.

A key advantage of surface brightness methods is their near independence from errors in the interstellar extinction. We showed that an error of 0.10 mag. in $E(B - V)$ leads to errors in distance, angular diameter, and radius of +0.2%, +0.4%, and +0.6%, respectively. On the other hand, the same error leads to a change in the distance determined through the Cepheid PL relation of -17% .

The final check we presented was to determine whether our use of a phase shift between

the photometry and the radial velocities had an affect on the distances and radii obtained. We performed all our calculations afresh with $\Delta\theta$ fixed at zero. The distances with $\Delta\theta = 0$ were found to be $0.4\% \pm 0.6\%$ larger in the mean than those with $\Delta\theta = \text{variable}$, which is entirely negligible. The radii showed a similar insensitivity.

From our sample of thirteen Cepheids we determined period-radius and period-luminosity relations. The radii we found for EU Tau and SZ Tau show strong support for interpreting them as overtone pulsators, and, in the case of EU Tau, strong support for theoretical models without convective overshoot. (The radius of SZ Tau agrees with prediction from models without convective overshoot, but its uncertainty precludes a definitive statement.) From all thirteen Cepheids we determined PR and PL relations

$$\log(\langle R \rangle) = 0.693(\pm 0.037)(\log(P) - 1.2) + 2.042(\pm 0.047), \quad (31)$$

$$\langle M_v(int) \rangle = -2.690(\pm 0.169)(\log(P) - 1.2) - 4.699(\pm 0.216) \quad (32)$$

As a check on these results we compared them to consensus relations from the recent literature, *ie*,

$$\log(\langle R \rangle) = 0.690(\pm 0.018)(\log(P) - 1.2) + 1.979(\pm 0.006), \quad (33)$$

$$\langle M_v(int) \rangle = -2.851(\pm 0.056)(\log(P) - 1.2) - 4.812(\pm 0.058) \quad (34)$$

An additional check is to compare our predicted absolute magnitude for δ Cep to that obtained by Benedict *et al.* (2002) from an HST parallax. Our PL relation predicts -3.43 ± 0.10 mag compared to -3.47 ± 0.10 mag. given by Benedict *et al.*.

We conclude that our Bayesian analysis is a powerful tool for determining properties and distances for Cepheid variables through the surface brightness technique.

We thank L. Szabados for assistance in period selection for these stars. We thank Pawel Moskalik for pointing us to several useful radial velocity papers. Electronic data transfers were generously provided by N. Samos and L. Berdnikov and were greatly appreciated. Binary velocity corrections for T Mon were made possible by computer code provided by Jos Tomkin, whom we thank for his help. This research made use of the McMaster Cepheid Photometry and Radial Velocity Archive at <http://www.physics.mcmaster.ca/Cepheid/> which is maintained by D.L. Welch and is supported, in part, by the Natural Sciences and Engineering Research Council of Canada (NSERC).

REFERENCES

- Alcock, C., Allsman, R. A., Axelrod, T. S., Bennett, D. P., Cook, K. H., Freeman, K. C., Griest, K., Marshall, S. L., Peterson, B. A., Pratt, M. R., Quinn, P. J., Reimann, J., Rodgers, A. W., Stubbs, C. W., Sutherland, W. & Welch, D. L. 1995, *AJ*, 109,1653
- Arellano Ferro, A., & Rosenzweig, P. 2000, *MNRAS*, 315, 296
- Barnes, T. G., Dominy, J. F., Evans, D. S., Kelton, P. W., Parsons, S. B., & Stover, R. J. 1977, *MNRAS*, 178, 661
- Barnes, T. G., & Evans, D. S. 1976, *MNRAS*, 174, 489
- Barnes, T. G., Evans, D. S., & Parsons, S. B. 1976, *MNRAS*, 174, 503
- Barnes, T. G., Fernley, J. A., Frueh, M. L., Navas, J. G., Moffett, T. J., & Skillen, I. 1997, *PASP*, 109, 645
- Barnes, T. G. & Jefferys, W. H. 1999, in *Harmonizing Cosmic Distance Scales in a Post-Hipparcos Era*, ed. D. Egret & A. Heck, *PASP Conf. Series*, 167, 243
- Barnes, T. G., Moffett, T. J., & Slovak, M. H. 1988, *ApJS*, 66, 43
- Barnes, T. G., Moffett, T. J., & Slovak, M. H. 1987, *ApJS*, 65, 307
- Benedict, G. F., McArthur, B. E., Fredrick, L. W., Harrison, T. E., Slesnick, C. L., Rhee, J., Patterson, R. J., Skrutskie, M. F., Franz, O. G., Wasserman, L. H., Jefferys, W. H., Nelan, E., van Altena, W., Shelus, P. J., Hemenway, P. D., Duncombe, R. L., Story, D., Whipple, A. L., & Bradley, A. J. 2002, *AJ*, 124, 1695
- Berdnikov, L.N., 1993, *Pis'ma Astr. Zh.*, 19, 210-263; *Astr. Letters*, 19, 84-97, 1993 translated
- Berdnikov, L. N. 1992a, *Astron. & Astrophys. Trans.*, 2, 1-30
- Berdnikov, L. N. 1992b, *Astron. & Astrophys. Trans.*, 2, 31-41
- Berdnikov, L. N. 1992c, *Astron. & Astrophys. Trans.*, 2, 43-105
- Berdnikov, L. N. 1992d, *Astron. & Astrophys. Trans.*, 2, 107-156
- Berdnikov, L. N. 1992e, *Astron. & Astrophys. Trans.*, 2, 157-181
- Berdnikov, L. N. 1992f, *Pis'ma Astr. Zh.*, 18, 325-374; *Astr. Letters*, 18, 130-142, 1992 translated

- Berdnikov, L. N. 1987, *Perem. Zvezdy*, 22, 530-548
- Berdnikov, L. N. 1986, *Perem. Zvezdy*, 22, 369-400
- Berdnikov, L. N., Ignatova, V. V., & Vozyakova, O. V. 1998, *Astron. & Astrophys. Trans.*, 17, 87-178
- Berdnikov, L. N., Ignatova, V. V., & Vozyakova, O. V. 1997, *Astron. & Astrophys. Trans.*, 14, 237-330
- Berdnikov, L. N., & Turner, D. G. 2000, *Astron. & Astrophys. Trans.*, 18, 679-749
- Berdnikov, L. N., & Turner D. G. 1995a, *Pis'ma Astr. Zh.*, 21, 603-632; *Astr. Letters*, 21, 534-564, 1995 translated
- Berdnikov, L. N., & Turner, D. G. 1995b, *Pis'ma Astr. Zh.*, 21, 803-871; *Astr. Letters*, 21, 717-785, 1995 translated
- Berdnikov, L. N., & Vozyakova, O. V. 1995, *Pis'ma Astr. Zh.*, 21, 348-378; *Astr. Letters*, 21, 308-338, 1995 translated
- Berdnikov, L. N., & Yakubov, S. D. 1993, *Perem. Zvezdy*, 23, 47-48
- Bersier, D., Burki, G., Mayor, M., & Duquennoy, A. 1994, *A&AS*, 108, 25
- Bono, G., Caputo, F., & Marconi, M. 1998, *ApJ*, 497, L43
- Bono, G., Gieren, W. P., Marconi, M., & Fouqué, P. 2001, *ApJ*, 552, L141
- Caldwell, J. A. R., Coulson, I. M., Dean, J. F., & Berdnikov, L. N. 2001, *Journal of Astr. Data*, 7, 4
- Carlin, B. P. & Chib, S. 1995, *Jour. Roy. Statist. Soc. B*, 57, 473
- Cardelli, J. A., Clayton, G. C., & Mathis, J. S. 1989, *ApJ*, 345, 245
- Casella, G., & George, E. I. 1992, *American Statistician*, 46, 167–174
- Chib, S., & Greenberg, E. 1995, *American Statistician* 49, 327–335
- Coulson, I. M., & Caldwell, J. A. R. 1985, *SAAO Circulars*, 9, 5
- Dellaportas, P., Forster, J., & Ntzoufras, I. 2002, *Statistics and Computing*, 12, 27
- Evans, N. R. 1984, *ApJ*, 28, 760

- Evans, N. R., Carpenter, K., Robinson, R., Massa, D. Wahlgren, G. M., Vinkó, J. & Szabados, L. 1999, ApJ, 524, 379
- Feast, M. W. 1999, PASP, 111,775
- Fernie, J. D. 1990, ApJS, 72,153
- Fernie, J. D., Beattie, B., Evans, N. R., & Seager, S. 1995, IBVS No. 4148
- Fouqué, P., & Gieren, W. P. 1997, A&A, 320, 799
- Freedman, W. L., Madore, B. F., Gibson, B. K., Ferrarese, L., Kelson, D. D., Sakai, S., Mould, J. R., Kennicutt, R. C., Ford, H. C., Graham, J. A., Huchra, J. P., Hughes, S. M. G., Illingworth, G. D., Macri, L.M. & Stetson, P. B. 2001, ApJ, 553, 47
- Gelfand, A. E., & Smith, A. F. M. 1990, Jour. Amer. Statist. Assn., 85, 398
- Gieren, W. 1981a, ApJS, 46, 287
- Gieren, W. 1981b, ApJS, 47, 315
- Gieren, W. P., Barnes, T. G., & Moffett, T. J. 1993, ApJ, 418, 135
- Gieren, W. P., Barnes, T. G., & Moffett, T. J. 1989a, ApJ, 342, 467
- Gieren, W. P., Fouqué, P., & Gómez, M. 1998, ApJ, 496, 17
- Gieren, W. P., Matthews, J., Moffett, T. J., Barnes, T. G., Frueh, M. L., & Szabados, L. 1989b, AJ, 98, 1672
- Gieren, W. P., Moffett, T. J., Barnes, T. G., Frueh, M. L., & Matthews, J. M. 1990 AJ, 99, 1196
- Gieren, W. P., Moffett, T. J., & Barnes, T. G. 1999, ApJ, 512, 553 (GMB)
- Gorynya, N. A., Irsambetova, T. R., Rastorguev, A. S., & Samus, N. N. 1992, Pis'ma Astr. Zh., 18, 777-801; Sov. Astr. Letters, 18, 316-324, 1992 translated
- Gorynya, N. A., Samus, N. N., Sachkov, M. E., Rasorguev, A. S., Glushkova, E. V., & Antipin, S. V. 1998, Pis'ma Astr. Zh., 24, 939-942; Astr. Letters, 24, 815-818, 1998 translated
- Gorynya, N. A., Samus, N. N., Rasorguev, A. S., & Sachkov, M. E. 1996, Pis'ma Astr. Zh., 22, 198-230; Astr. Letters, 22, 175-206, 1996 translated

- Green, P. J. 1995, *Biometrika*, 82, 711
- Groenewegen, A. J., & Oudmaijer, R. D. 2000, *A&A*, 356, 49
- Gull, S. F. 1988, in *Maximum Entropy and Bayesian Methods in Science and Engineering*, ed. Gary J. Erickson & C. Ray Smith (Dordrecht: Kluwer), 53–74
- Hindsley, R. B., & Bell, R. A. 1986, *PASP*, 98, 881
- Hoeting, J. A., Madigan, D., Raftery, A. E., & Volinsky, C. T. 1999, *Statistical Science* 14, 382
- Imbert, M. 1999, *A&AS*, 140, 79
- Johnson, H. L. 1968, in *Nebulae and Interstellar Matter*, ed. G. P. Kuiper & B. M. Middlehurst (Chicago: Univ. Chicago Press), 194
- Kiss, L. L. 1998, *MNRAS*, 297, 825
- Kiss, L. & Vinkó, J. 2000, *MNRAS*, 314, 420
- Laney, C. D. & Stobie, R. S. 1995, *MNRAS*, 274, 337
- Lloyd Evans, T. 1980, *SAAO Circulars*, 1, 257
- Loredo, T. J. 1990, in *Maximum Entropy and Bayesian Methods*, ed. Paul F. Fougère (Dordrecht: Kluwer), 81–142
- Luri, X., Torra, F., Figueras, F., Gómez, A. E., Goupil, M. J., & Beaulieu, J. P. 1999, in *Harmonizing Cosmic Distance Scales in a Post-Hipparcos Era*, ed. D. Egret & A. Heck, *PASP Conf. Series*, 167, 33
- Lutz, T. E., & Kelker, D. H. 1973, *PASP*, 85, 573
- Mermilliod, J. C., Mayor, M., & Burki, G. 1987, *A&AS*, 70, 389
- Moffett, T. J., & Barnes, T. G. 1985, *ApJS*, 58, 843
- Moffett, T. J., & Barnes, T. G. 1984, *ApJS*, 55, 389
- Nordgren, T. E., Lane, B. F., Hindsley, R. B., & Kervella, P. 2002, *AJ*, 123, 3380.
- Olson, B. I. 1975, *PASP*, 87, 349
- Ripepi, V., Barone, F., Milano, L., & Russo, G. 1997, *AA*, 318, 797

- Sachkov, M. E., Rastorguev, A. S., Samus, N. N., & Gorynya, N. A. 1998, *Astr. Letters*, 24, 377
- Smith, A. F. M., & Gelfand, A. E. 1992, *American Statistician* 46, 84–88
- Smith, H. 1999, in *Modern Astrometry and Astrodynamics*, ed. R. Dvorak, H. F. Haupt, & K. Wodnar (Vienna: Austrian Academy of Sciences), p. 139
- Szabados, L. 1991, *Comm. Konkoly Observatory*, No. 96.
- Szabados, L. 1989, *Comm. Konkoly Observatory*, No. 94.
- Szabados, L. 1977, *Comm. Konkoly Observatory*, No. 70.
- Taylor, B. J. 1986, *ApJS*, 60, 577
- Tierney, L. 1994, *Annals of Statistics*, 22, 1701
- Turner, D. G., & Burke, J. F. 2002, *AJ*, 124, 2931
- Welch, D. L. 1994, *AJ*, 108, 1421
- Wilson, T. D., Carter, M. W., Barnes, T. G., Van Citters, G. W., & Moffett, T. J. 1989, *ApJS*, 69, 951

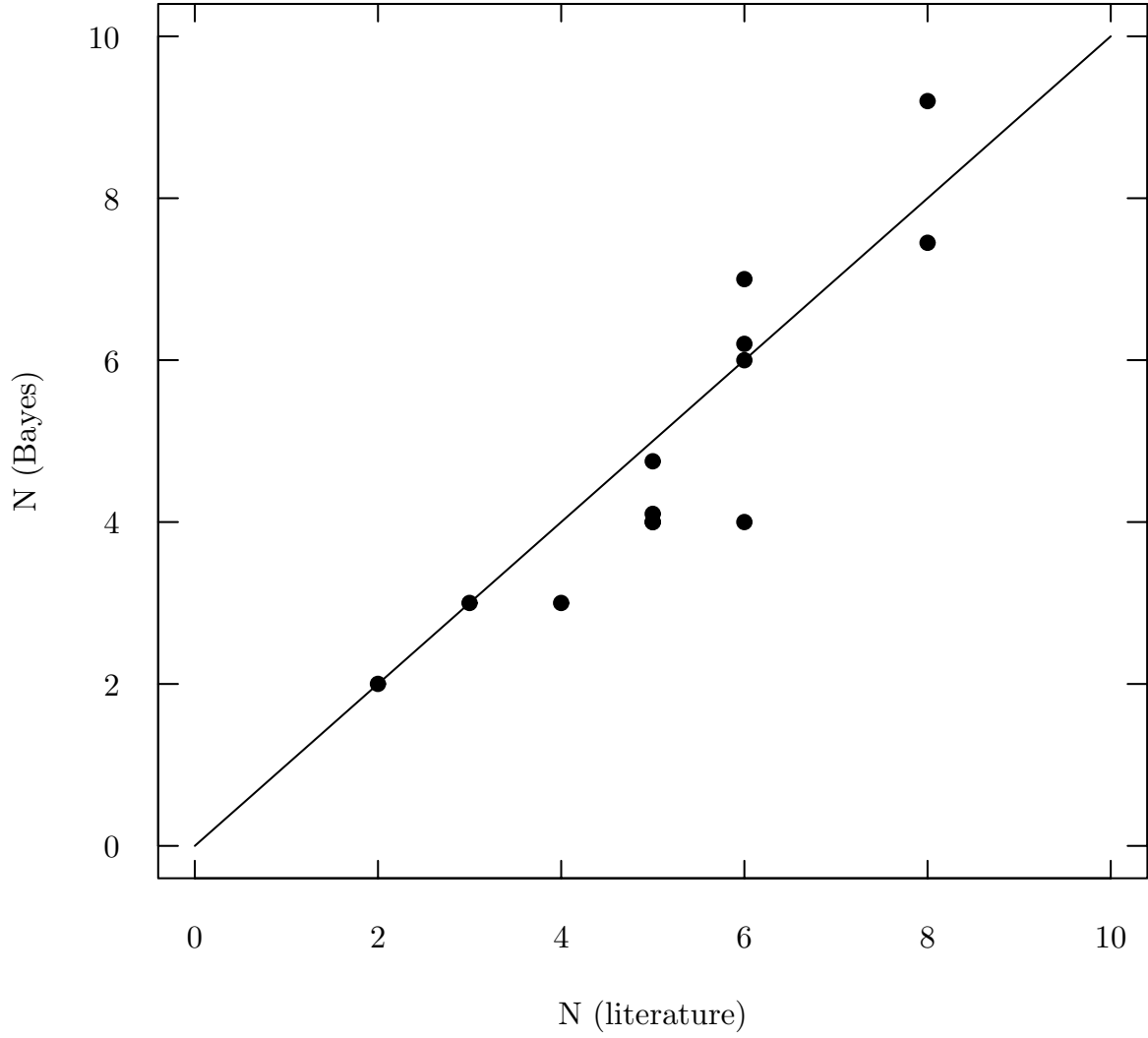


Fig. 1.— Comparison of V light curve Fourier orders from our Bayesian analyses with those from previous work. A line of equality is shown for illustration.

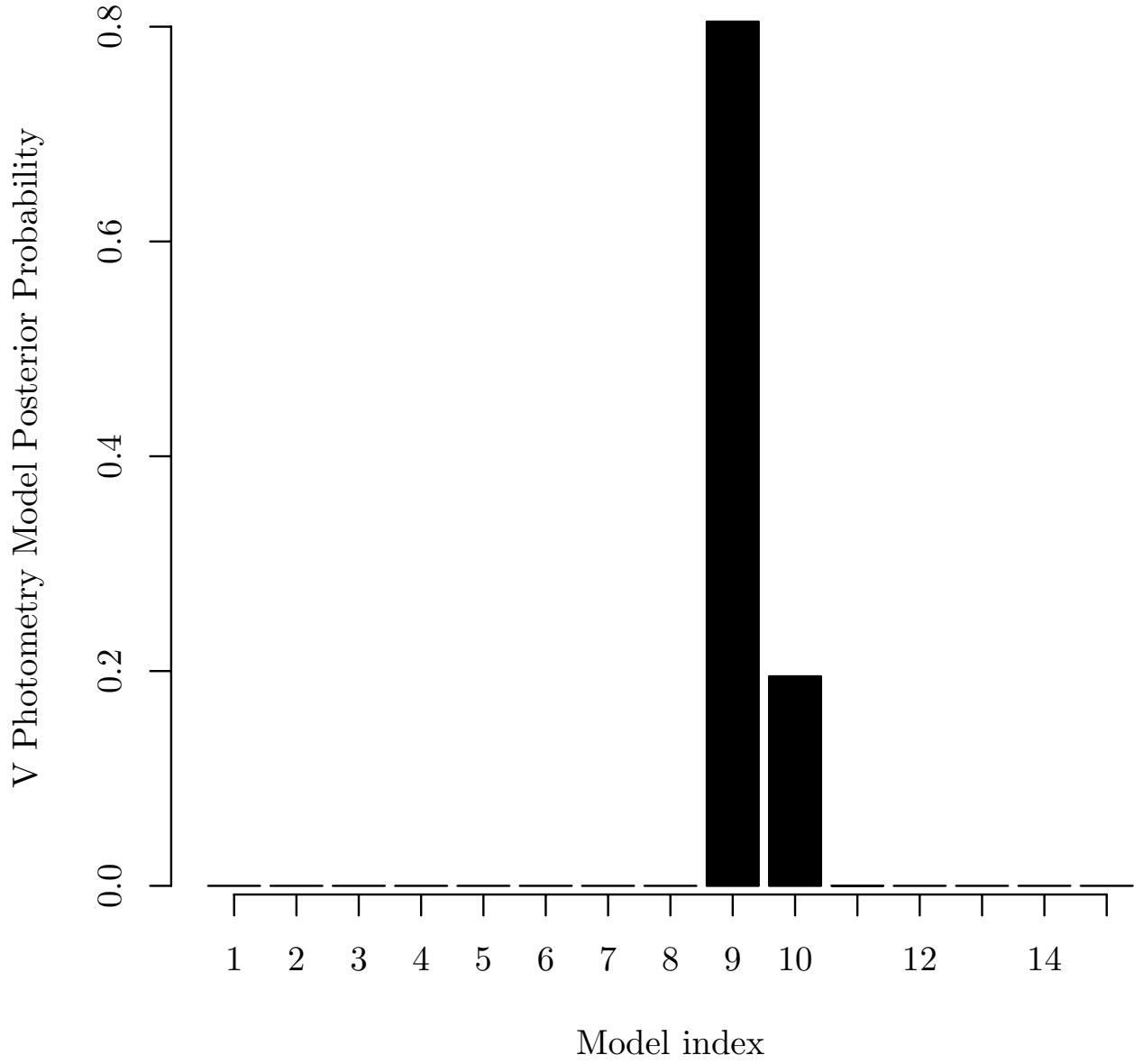


Fig. 2.— Posterior marginal distribution of photometry models for X Cyg.

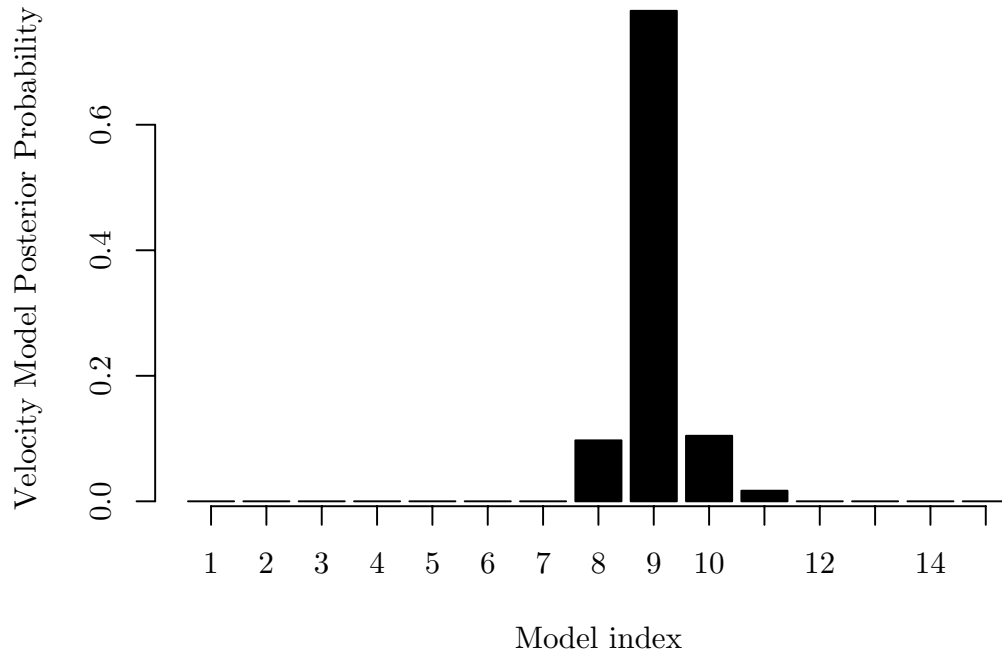


Fig. 3.— Posterior marginal distribution of velocity models for X Cyg.

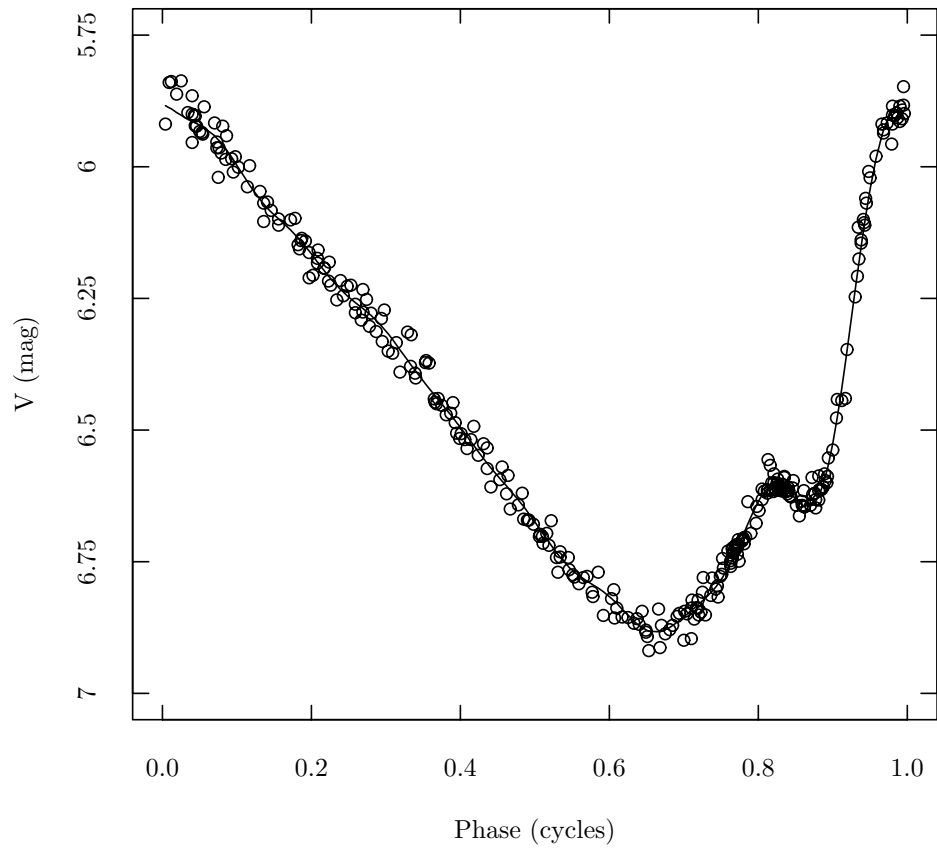


Fig. 4.— The V light curve for X Cyg. A Fourier polynomial of order $N = 9$ is shown fitted to the observations.

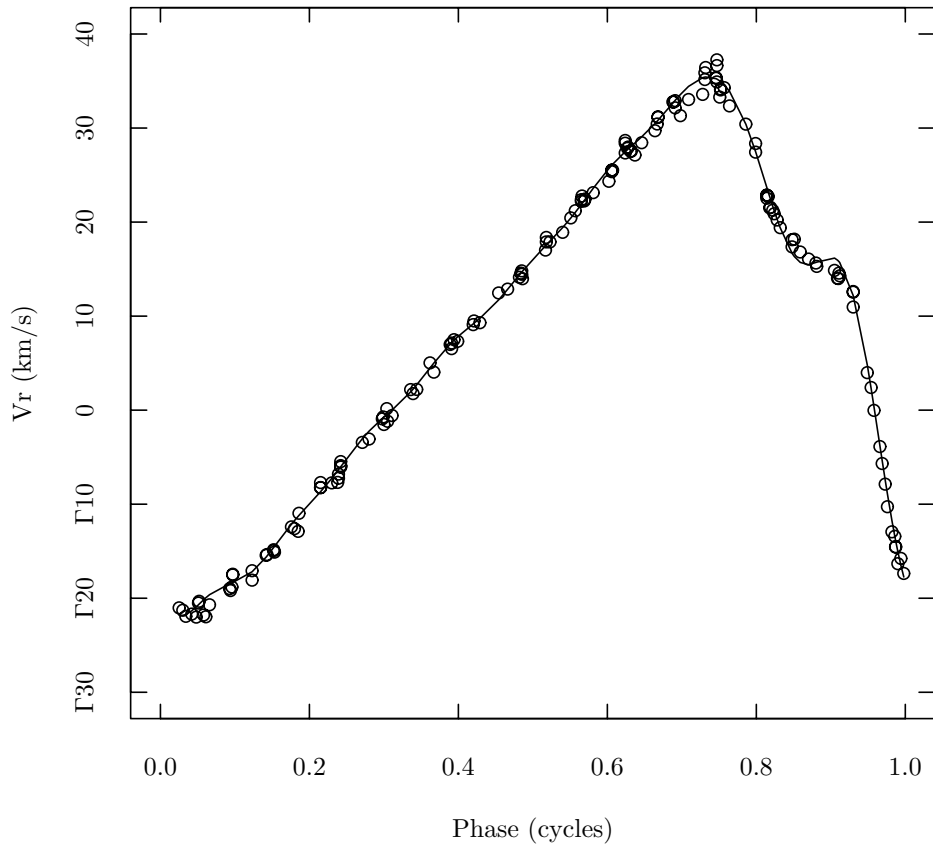


Fig. 5.— The radial velocity curve for X Cyg with low weight data suppressed for clarity. A Fourier polynomial of order $M = 9$ is shown fitted to the observations.

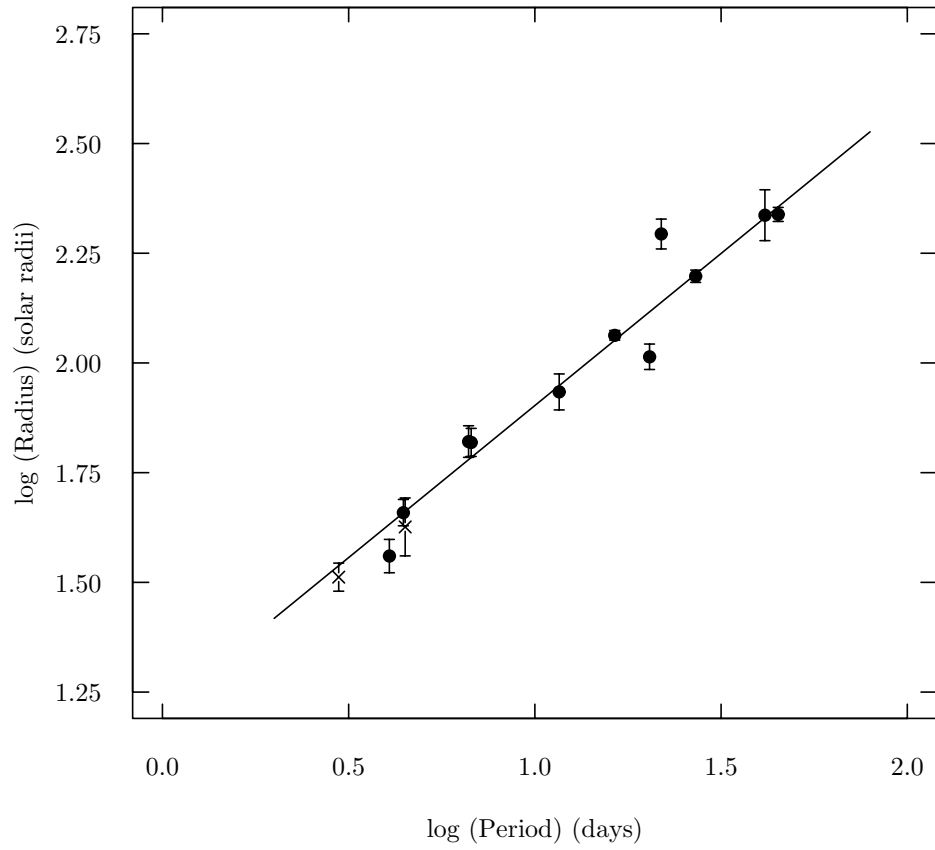


Fig. 6.— Period–Radius relation for our sample. Fundamental-mode Cepheids are plotted with filled symbols; SZ Tau and EU Tau are plotted as X symbols at their computed fundamental periods. The line shows the weighted, least-squares fit.

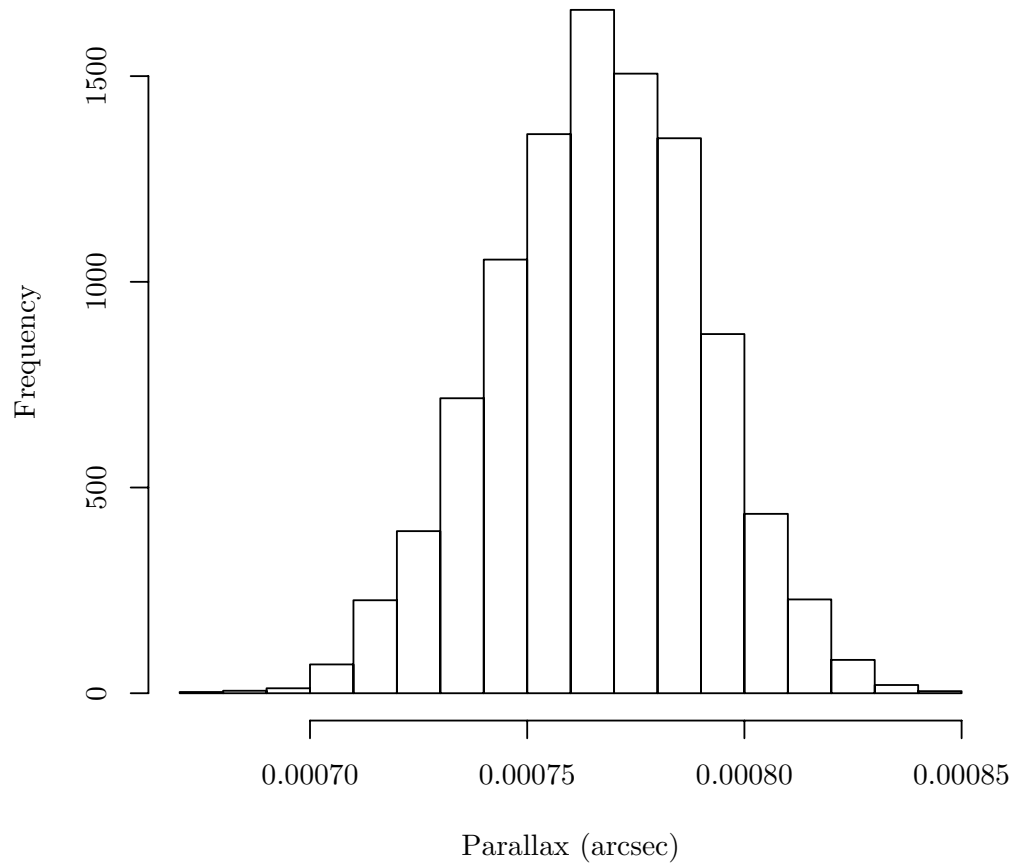


Fig. 7.— Posterior marginal distribution of the parallax of T Mon.

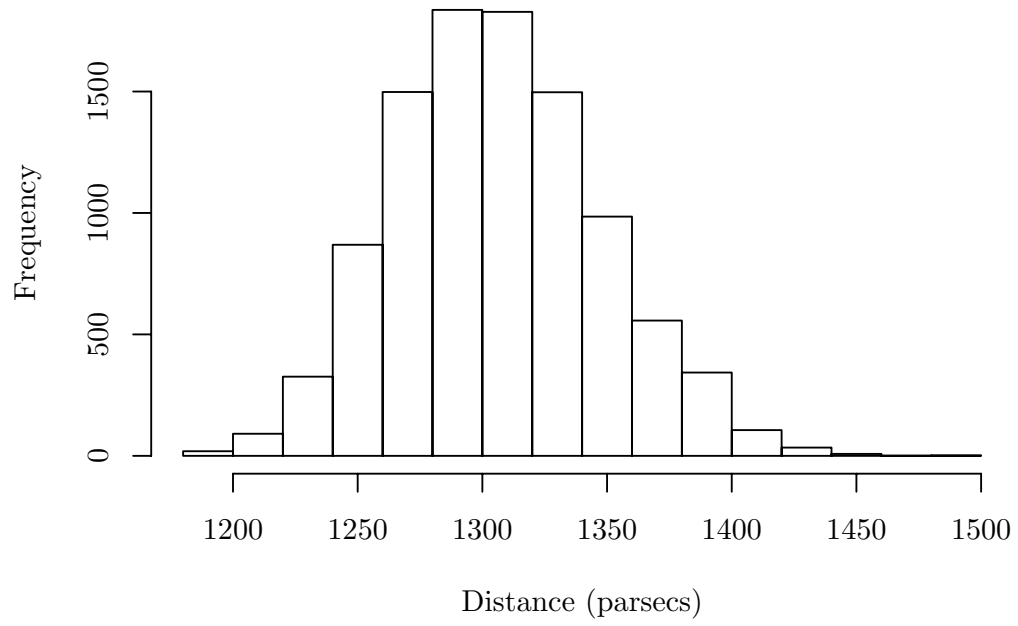


Fig. 8.— Posterior marginal distribution of the distance of T Mon.

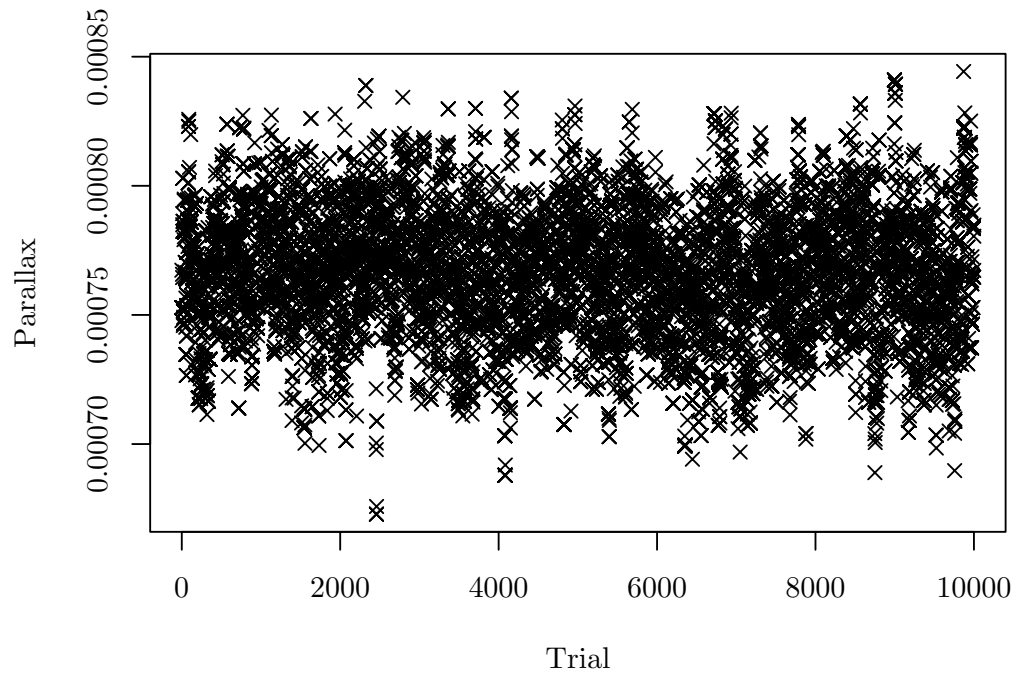


Fig. 9.— Simulation history of the parallax of T Mon.

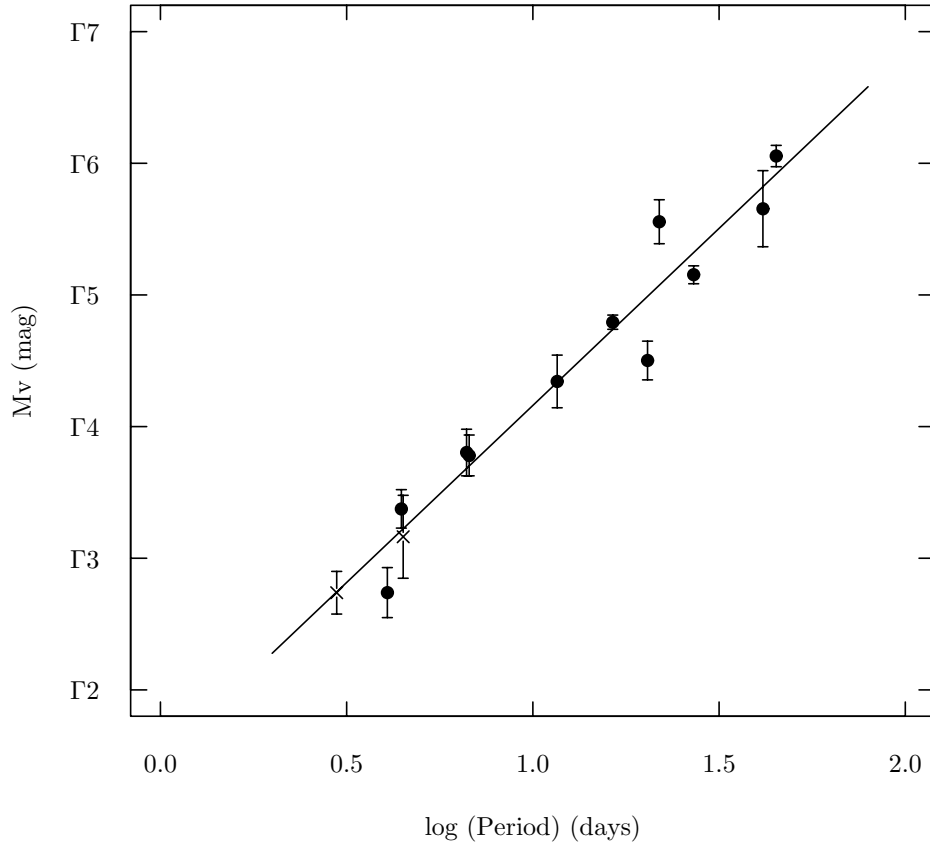


Fig. 10.— Period-luminosity relation for our results. The $\langle M_v(int) \rangle$ magnitudes of Table 6 are plotted against $\log(\text{period})$. Fundamental-mode Cepheids are plotted with filled symbols; SZ Tau and EU Tau are plotted as X symbols at their computed fundamental periods. The line shows the weighted, least-squares fit.

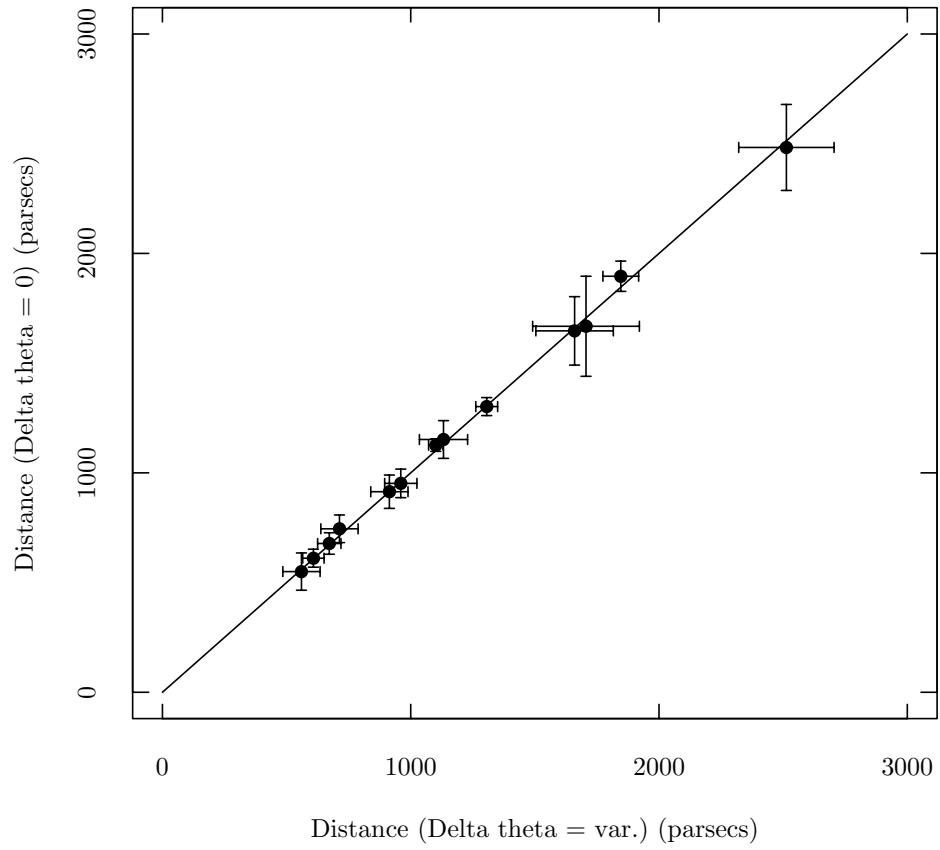


Fig. 11.— Distances determined with $\Delta\theta$ fixed at zero plotted against distances obtained with $\Delta\theta$ variable. A line of equality is shown for comparison.

Table 1. Adopted Parameters

Cepheid	$E(B - V)$ (mag)	Period (days)	Period Source
RX Aur	0.276	11.623837	Moffett & Barnes (1985)
X Cyg	0.288	16.385692	Szabados (1991)
T Mon	0.209	27.026	Evans <i>et al.</i> (1999)
BF Oph	0.247	4.067698	Szabados (1989)
RS Pup	0.446	41.467	This paper
U Sgr	0.403	6.745229	Szabados (1989)
WZ Sgr	0.467	21.849789	Szabados (1989)
BB Sgr	0.284	6.637005	Szabados (1989)
RY Sco	0.777	20.321044	Szabados (1989)
SZ Tau	0.294	3.14895	This paper
EU Tau	0.172	2.10248	Szabados (1977)
T Vul	0.064	4.435453	Szabados (1991)
SV Vul	0.570	45.019	This paper

Table 2. Data Sources

Cepheid	Photometric Values	Photometric Sources	Velocity Values	Velocity Sources
RX Aur	89	7,12,13,14,19,35	58	3,30,36
X Cyg	311	1,4,7,8,9,10,12,13,14,18,35	199	3,20,31,32,36
T Mon	181	4,6,7,10,12,15,17,18,22,35	144	3,20,23,32,36
BF Oph	183	5,6,8,9,13,15,21,25,35	52	3,24,33
RS Pup	81	15,17,35	26	2
U Sgr	330	4,7,8,9,10,11,12,13,14,15,16,17,18,21,25,35	156	3,20,24,31,34,36
WZ Sgr	150	7,12,13,14,22,35	104	2,22,28,29
BB Sgr	281	4,6,7,10,13,14,15,16,17,18,21,25,35	117	2,24,28,29,33
RY Sco	92	15,22,35	45	2,22,33
SZ Tau	77	1,35	149	3,20,27,28,29,31,
...	32,36
EU Tau	345	26	118	20,26,27,28,29
T Vul	305	1,4,5,6,7,8,9,10,13,14,18,35	190	3,20,32,32,36
SV Vul	374	1,4,5,6,7,8,10,11,12,13,14,18,35	162	3,20,30,32,36

References. — 1–Barnes *et al.* 1997, 2–Barnes, Moffett, & Slovak 1988, 3–Barnes, Moffett, & Slovak 1987, 4–Berdnikov 1993, 5–Berdnikov 1992a, 6–Berdnikov 1992b, 7–Berdnikov 1992c, 8–Berdnikov 1992d, 9–Berdnikov 1992e, 10–Berdnikov 1992f, 11–Berdnikov 1987, 12–Berdnikov 1986, 13–Berdnikov, Ignatova, & Vozyakova 1998, 14–Berdnikov, Ignatova, & Vozyakova 1997, 15–Berdnikov & Turner 2000, 16–Berdnikov & Turner 1995a, 17–Berdnikov & Turner 1995b, 18–Berdnikov & Vozyakova 1995, 19–Berdnikov & Yakubov 1993, 20–Bersier *et al.* 1994, 21–Caldwell *et al.* 2001, 22–Coulson & Caldwell 1985, 23–Evans *et al.* 1999, 24–Gieren 1981a, 25–Gieren 1981b, 26–Gieren *et al.* 1989b, 27–Gorynya *et al.* 1992, 28–Gorynya *et al.* 1998, 29–Gorynya *et al.* 1996, 30–Imbert 1999, 31–Kiss 1998, 32–Kiss & Vinkó 2000, 33–Lloyd Evans 1980, 34–Mermilliod, Mayor, & Burki 1987, 35–Moffett & Barnes 1984, 36–Wilson *et al.* 1989

Table 3. Diagnostic Results

Cepheid	$\Delta\theta$	$\sigma_{\Delta\theta}$	N Photometry	M Velocities	$\sqrt{\tau_V}$ V	$\sqrt{\tau_C}$ (V – R)	$\sqrt{\tau_U}$ Velocity
RX Aur	–0.0014	± 0.0152	4,5	3	0.82	0.84	0.82
X Cyg	–0.0210	± 0.0039	9,10	9,10,8	0.68	0.93	0.57
T Mon	0.0194	± 0.0045	6,7	8	0.59	0.78	0.55
BF Oph	–0.0489	± 0.0128	4	3,2	0.46	0.58	1.26
RS Pup	0.0102	± 0.0199	4	3,4	0.17	0.56	0.55
U Sgr	–0.0294	± 0.0111	7	5,7	0.52	0.73	0.75
WZ Sgr	0.0237	± 0.0127	7,8	7,8,9	0.46	0.56	0.33
BB Sgr	–0.0190	± 0.0122	3	4	0.30	0.63	0.45
RY Sco	0.0135	± 0.0100	5,4	1,2	0.46	0.89	0.82
SZ Tau	–0.0031	± 0.0219	2	2	1.39	0.68	0.23
EU Tau	–0.0625	± 0.0124	3	3,2	0.53	0.70	0.51
T Vul	–0.0215	± 0.0103	4	4,5	0.50	0.72	0.44
SV Vul	–0.0289	± 0.0052	6	4,3	0.33	0.70	0.13
Mean of 13	–0.0115	± 0.0065			0.55 ± 0.08	0.72 ± 0.03	0.57 ± 0.08
Mean of 7	–0.0034	± 0.0099					

Table 4. Radius Results

Cepheid	$\langle R \rangle$ Solar radii	σ_R Solar radii	$\langle \phi \rangle$ milliarcsec	σ_ϕ milliarcsec
RX Aur	85.9	± 8.1	0.4514	± 0.0016
X Cyg	115.6	± 2.8	0.9166	± 0.0017
T Mon	157.6	± 4.9	1.0531	± 0.0022
BF Oph	36.3	± 3.2	0.4443	± 0.0013
RS Pup	217.1	± 29.0	1.1106	± 0.0063
U Sgr	65.9	± 4.8	0.8548	± 0.0020
WZ Sgr	196.7	± 15.3	0.6831	± 0.0028
BB Sgr	66.2	± 5.4	0.6315	± 0.0014
RY Sco	103.3	± 7.0	0.9394	± 0.0032
SZ Tau	42.3	± 6.4	0.6593	± 0.0012
EU Tau	32.5	± 2.4	0.2507	± 0.0002
T Vul	45.6	± 3.1	0.6547	± 0.0013
SV Vul	218.0	± 8.1	1.0306	± 0.0025

Table 5. Cepheid Period–Radius Relations

Slope	Zero Point	Type	Source
0.693 ± 0.037	2.042 ± 0.047	(V-R)	This paper
0.737 ± 0.028	1.984 ± 0.025	KHG	Turner & Burke (2002)
0.649 ± 0.051	1.953 ± 0.042	(b-y)	Arellano Ferro & Rosenzweig (2000)
0.680 ± 0.017	1.962 ± 0.025	(V-R), (J-K)	Gieren, Moffett, & Barnes (1999)
0.655 ± 0.006	1.974 ± 0.008	Theory*	Bono, Caputo, & Marconi (1998)
0.750 ± 0.023	1.975 ± 0.028	(J-K)	Gieren, Fouqué, & Gómez (1998)
0.610 ± 0.030	1.980 ± 0.03	(B-V), (V-R)	Sachkov, Rastorguev, Samus, & Gorynya (1998)
0.606 ± 0.037	1.990 ± 0.033	CORS	Ripepi, Barone, Milano, & Russo (1997)
0.741 ± 0.026	1.985 ± 0.031	(J-K)	Laney & Stobie (1995)
0.690 ± 0.018	1.979 ± 0.006	...	Weighted mean of nine solutions
* models with $Z = 0.02$, no convective overshoot			

Table 6. Overtone Cepheid Radii

	EU Tau	SZ Tau
Period (days)	2.10248	3.14895
$\langle R \rangle$ Table 4	32.5 ± 2.4	42.3 ± 6.4
$\langle R \rangle^*$ no overshoot	31.2	42.2
$\langle R \rangle^*$ with overshoot	28.6	38.6
$\langle R \rangle$ from Eq. 25	23.6	31.2

* radii from Bono *et al.* (2001)

Table 7. Distance Results

Cepheid	s parsecs	π milliarcsec	$\langle M_V(mag) \rangle$ mag	$\langle M_V(int) \rangle$ mag
RX Aur	1660 ± 156	0.6076 ± 0.0553	-4.322 ± 0.200	-4.343 ± 0.200
X Cyg	1101 ± 28	0.9092 ± 0.0227	-4.744 ± 0.054	-4.793 ± 0.054
T Mon	1306 ± 41	0.7664 ± 0.0241	-5.100 ± 0.068	-5.153 ± 0.068
BF Oph	713 ± 63	1.4133 ± 0.1226	-2.718 ± 0.190	-2.739 ± 0.190
RS Pup	1706 ± 228	0.5966 ± 0.0794	-5.597 ± 0.288	-5.655 ± 0.289
U Sgr	672 ± 49	1.4951 ± 0.1050	-3.756 ± 0.155	-3.781 ± 0.155
WZ Sgr	2513 ± 196	0.4003 ± 0.0304	-5.494 ± 0.167	-5.556 ± 0.167
BB Sgr	914 ± 76	1.1011 ± 0.0883	-3.786 ± 0.176	-3.803 ± 0.176
RY Sco	960 ± 65	1.0469 ± 0.0712	-4.466 ± 0.147	-4.502 ± 0.147
SZ Tau	560 ± 85	1.8239 ± 0.2566	-3.156 ± 0.315	-3.163 ± 0.315
EU Tau	1132 ± 86	0.8882 ± 0.0659	-2.732 ± 0.162	-2.738 ± 0.162
T Vul	608 ± 41	1.6515 ± 0.1109	-3.354 ± 0.146	-3.375 ± 0.146
SV Vul	1846 ± 69	0.5425 ± 0.0201	-6.003 ± 0.081	-6.055 ± 0.081

Table 8. Cepheid Period–Luminosity Relations

Slope	Zero Point	Type	Source
-2.690 ± 0.169	-4.699 ± 0.215	(V-R)	This paper
-2.694 ± 0.138	-4.657 ± 0.132	KHG	Turner & Burke (2002)
-2.810 ± 0.060	-4.820 ± 0.090	Hipparcos π	Feast (1999)
-3.037 ± 0.138	-4.665 ± 0.164	(J-K)	Gieren, Fouqué, & Gómez (1998)
-2.986 ± 0.094	-4.954 ± 0.095	(V-R)	Gieren, Barnes, & Moffett (1993)
-2.851 ± 0.056	-4.812 ± 0.058	...	Weighted mean of five solutions

Table 9. Absolute Magnitude of δ Cep

Source	M_v mag	Difference mag
Benedict <i>et al.</i> (2002)	-3.47 ± 0.10	...
Nordgren <i>at al.</i> (2002)	-3.55 ± 0.08	-0.08 ± 0.13
PL relation this paper, Eq. 27	-3.43 ± 0.10	0.04 ± 0.14
Mean PL relation, Eq. 28	-3.47 ± 0.06	0.00 ± 0.12
Freedman <i>et al.</i> (2001)	-3.47 ± 0.03	0.00 ± 0.10